Faculty of
Industrial Technology
Universitas Pertamina

Universitas Pertamina

Journal of

Emerging Supply Chain, Clean Energy, and Process Engineering

Vol 3, No 1, 2024

Journal of

Emerging Supply Chain, Clean Energy, and Process Engineering

Vol 3, No 1, 2024

5. Assoc. Prof. Agustian Taufiq Asyhari (Scopus ID: 24330878400, School of Computing and Digital Technology, Birmingham City University, United Kingdom)

6. Assoc. Prof. Karar Mahmoud (Scopus ID: 36181590200, Department of Electrical Engineering, Aswan University, Egypt)

7. Asst. Prof. Ramon Zamora (Scopus ID: 35773032600, School of Engineering, Computer and Mathematical Sciences, Auckland University of Technology, New Zealand)

8. Asst. Prof. Wahyu Caesarendra (Scopus ID: 33067448100, Faculty of Integrated Technologies, Universiti Brunei Darussalam, Brunei Darussalam)

9. Asst. Prof. Miftakhul Huda (Scopus ID: 36782282400, Graduate School of Engineering, Chemical Systems Engineering, Nagoya University, Japan)

10. Choiru Za'in, Ph.D (Scopus ID: 57193255433, Lecturer, Department of Computer Science and Information Technology, La Trobe University)

11. Asst. Prof. Ahmed Bedawy Khalifa Hussein (Scopus ID: 54924520900, Department of Electrical Engineering, South Valley University, Egypt)

Journal of

Emerging Supply Chain, Clean Energy, and Process Engineering

Vol 3, No 1, 2024

Reviewers

1. Dr. Dr. Eng. Imam Wahyudi Farid, S.T., M.T. (Institut Teknologi Sepuluh Nopember, Indonesia)
2. Dr. Eng. Aditya Tirta Pratama, S.Si., M.T. (Swiss German University, Indonesia)
3. Dr. Eng. Muhammad Abdillah, S.T., M.T. (Universitas Pertamina, Indonesia)
4. Dr. Eng. Rizal Mahmud, S.Pd., M.T. (Badan Riset dan Inovasi Nasional (BRIN), Indonesia)
5. Dr. Eng. Iwan Sukarno, ST., M.Eng., CLIP (Universitas Pertamina, Indonesia)
6. Dr. Eng. Muhammad Kozin, S.T., M.Si. (Badan Riset dan Inovasi Nasional (BRIN), Indonesia)
7. Dr. Eng. Agus Susanto, S.Pd., M.T. (Politeknik Negeri Madiun, Indonesia)

Imprint

Postal Address

Journal of

Emerging Supply Chain, Clean Energy, and Process Engineering

Vol 3, No 1, 2024

PREFACE

The Journal of Emerging Supply Chain, Clean Energy and Process Engineering (JESCEE) is a journal of the Faculty of Industrial Technology, Universitas Pertamina that promotes communication between researchers, dissemination of research results, development of academic culture, and development of new ideas in the fields of mechanical, electrical, chemical, and logistics. This journal's volume 3, issue no. 1 has captivated the attention of numerous researchers interested in publishing their work.

On behalf of the Editor-in-Chief, I would like to thank the people who support this journal, especially the Dean of the Faculty of Industrial Technology Industrial for their direct and indirect assistance, the editors who work well and are dedicated, the reviewers who provide suggestions and constructive criticism for each paper collected, and the authors who entrust JESCEE with the publication of their research results.

We hope that this publication will continue to expand and present the most recent information in the fields of mechanical, electrical, chemical, and logistical. We also welcome collaboration from parties who are pleased with the existence of this journal and wish for its further growth.

Jakarta, June 2024
Editor-in-Chief

Dr. Eng. Muhammad Abdillah

Journal of

Emerging Supply Chain, Clean Energy, and Process Engineering

Vol 3, No 1, 2024

List of Contents

SUM-DIFFERENCE METHOD IN MONOPULSE RADAR: A REVIEW

Alam[1], Syahfrizal Tahcfulloh[1*]
[1]Department of Electrical Engineering, Universitas Borneo Tarakan, Indonesia

Abstract
This article reviews the sum and difference methods on monopulse radar used to detect targets during the tracking process. These methods are described in detail and comprehensively regarding optimizing the size of the subarray elements, optimizing the radiation energy of tracking targets, optimizing for obtaining lower sidelobe level and optimizing computations for digital processing. Considerations of potential strategies for configuring an implementable monopulse radar are also given. This article also provides answers when faced with the challenge of building a monopulse subarray radar that meets the implementation needs of both software and hardware. The expected result of this subarray on monopulse radar is to obtain flexible and general capabilities for detection and tracking that can adapt to target and environmental conditions, including countering interference and jamming.

1. Introduction

The aim of this paper is to review the methods that have been proposed to improve performance and explore the development potential of monopulse radar. In general, monopulse radar is used to detect targets using beam sum and difference. The monopulse angle estimation technique is used to determine the target location during the target tracking process [1]. By comparing different signals received by two or more antennas simultaneously, monopulse radar can obtain angular information from the target. The monopulse ratio of a detection target is determined based on the ratio of the beam sum to the difference in the target location. Ideally the characteristic curve of the monopulse ratio is linear. To calculate the monopulse ratio, the beam sum and difference must be formed simultaneously and at the same time the sidelobe level (SLL) in both beams must also be suppressed [2]-[11]. There are two monopulse radar techniques for obtaining information about the angle of the target from the reflected signal, i.e., amplitude comparison and phased-comparison. In amplitude comparison, determining the pattern sum and difference is obtained from the beam amplitudes of two or more adjacent beams, so that to estimate the target angle it is necessary to determine the sum beam, horizontal difference beam (elevation direction information), and vertical difference beam (azimuth direction information). In amplitude comparison, the two beams have the same phase [14][22].

Based on the structure of the radar antenna array, monopulse radar is divided into monopulse phased array (PA) radar [1]-[7], monopulse multiple-input multiple-output (MIMO) radar [12]-[20], and/or monopulse subarray radar [21]-[31]. PA radar is a radar whose antenna elements are arranged closely spaced where the coherent gain obtained is high so that it is appropriate for tracking radar targets. There are three types of PA radar used, namely uniform linear array (ULA) [1][3], uniform planar array [2][5][7], and non-uniform planar array [4]. Accurate target location determination is determined by monopulse estimation radar PA through monopulse slope design and calculation using the Cramér-Rao bound (CRB) method [1]. There is also a monopulse ratio calculation on the planar PA radar which is used to determine two-dimensional target locations (elevation and azimuth) and is equipped with mainlobe jamming cancellation to increase target detection accuracy [2]. A study that proposes adaptive beamforming on ULA with interference cancellation so as to increase the monopulse ratio has been proposed by [3]. Likewise, the use of a nonuniform planar array with phased comparison monopulse produces performance that is as good as a uniform planar array, which has been reported by [4]. If the size of the antenna array is very large, it is necessary to adjust the excitation elements periodically so that it is more reliable and consistent in forming the desired sidelobe pattern as reported by [5]. Apart from setting the excited elements, it is also necessary to optimize them to produce a sum beam with maximum slope in the boresight (target) direction

and optimally lowering the sidelobe envelope [6]. A study by [7] has reported that for fixed planar arrays it is necessary to design a pattern of sum and difference so that the radiation performance is maximum, such as field slope, amplitude, directivity and lower sidelobe.

For MIMO radar, the diversity gain will be explored because usually the antenna elements in transmit-receive are widely separated so they will have different angle values when viewing the target, especially related to the reflection coefficient of the target. In the research presented in [12], a technique is needed that is created using a 3-dimensional distributed array antenna on a MIMO radar so that a very narrow beam is formed. Apart from that, several advantages of MIMO radar compared to PA radar are the increase in spatial degree of freedom and detection/estimation probability [13]. According to [14] that the use of multiple widely separated antennas will provide significant improvements in spatial diversity compared to PA radar. Multiple widely separated antennas can also be equipped with frequency diversity, spatial diversity, and polarization diversity so that they are able to mitigate angular glints and at the same time increase the amount of energy in the reflected signal from the detection target [15]. The use of orthogonal waveform transmission will increase angular resolution in coherent MIMO scenarios and higher detection probability in statistical MIMO scenarios [16].

The monopulse subarray structure usually uses PA radar as its constituent and is non-overlapped. The types of subarrays are linear arrays [21]-[22], [28]-[31], uniform planar arrays [23]-[25], and nonuniform arrays [26] as shown in Fig. 1. The general purpose of using subarrays in monopulse radar is to reduce hardware costs and circuit complexity, making it easier for digital processing [21]-[23], to optimize subarray excitation with various methods [24]-[26], overcome beam shape loss and suppress jamming. and interference [27][31], maximizing directivity [28], and minimizing sidelobe levels [29][30].

Based on the literature used in this paper, the monopulse subarray method is widely used in uniform array radars, both linear arrays and planar arrays. To obtain information on the angle of the detection target in the elevation and azimuth directions, a planar array is used. Monopulse with AC is more attractive and simple to implement compared to PC. However, when using subarrays in monopulse radar, you must also consider things such as subarray element size, subarray excitation, maximum directivity, lower SLL to minimize the effect of interference and jamming, simplifying the computing time of digital processing, and considering implementation costs.

2. Method

This section provides an explanation of the monopulse radar signal model, existing methods for this radar and potential strategies for implementing this radar including its challenges.

A. Monopulse Radar Signal Model

In this section, a general illustration for monopulse radar will be given so as to provide systematic thinking about things that need to be developed in monopulse radar. If it is assumed that there are K antenna elements grouped into N-subarrays as shown in Figs. 1(a)-(b) where Fig. 1(a) for uniform and uniform subarrays the number of elements per subarray and Fig. 1(b) for varying subarrays. The weighting at the analog level is called $\mathbf{w}_k$ with $k = 1, 2, ..., K$ and there are two types of weighting at the digital level, i.e., subarray weighting for beam difference azimuth and elevation respectively, i.e., w_{sn}^a and w_{sn}^e with $n = 1, 2, ..., N$. Meanwhile, the beampattern sum is Σ and the beampattern difference angles of azimuth (φ) and elevation (θ) are Δ_a and Δ_e, respectively. If it is stated that the transformation operation of elements into subarrays is non-overlapped, it is expressed by the following $K \times N$ dimensional matrix $\mathbf{T}$ [23]

$$\mathbf{T} = diag(\mathbf{\psi} \circ \mathbf{w}_k)\mathbf{T}_o \tag{1}$$

where $\circ$ is the Hadamard product, $diag(\cdot)$ is the diagonal matrix, $\mathbf{\psi}$ is the analog phase shifting vector, $\mathbf{w}_k$ is the amplitude tapering on the k-th antenna element, and $\mathbf{T}_o$ is the transformation subarray matrix which is given a value, i.e.,

$$[\mathbf{T}_o]_{kn} = \begin{cases} 1 & k\text{th element} \in n\text{th subarray} \\ 0 & k\text{th element} \notin n\text{th subarray} \end{cases} \tag{2}$$

2

(a)

(b)
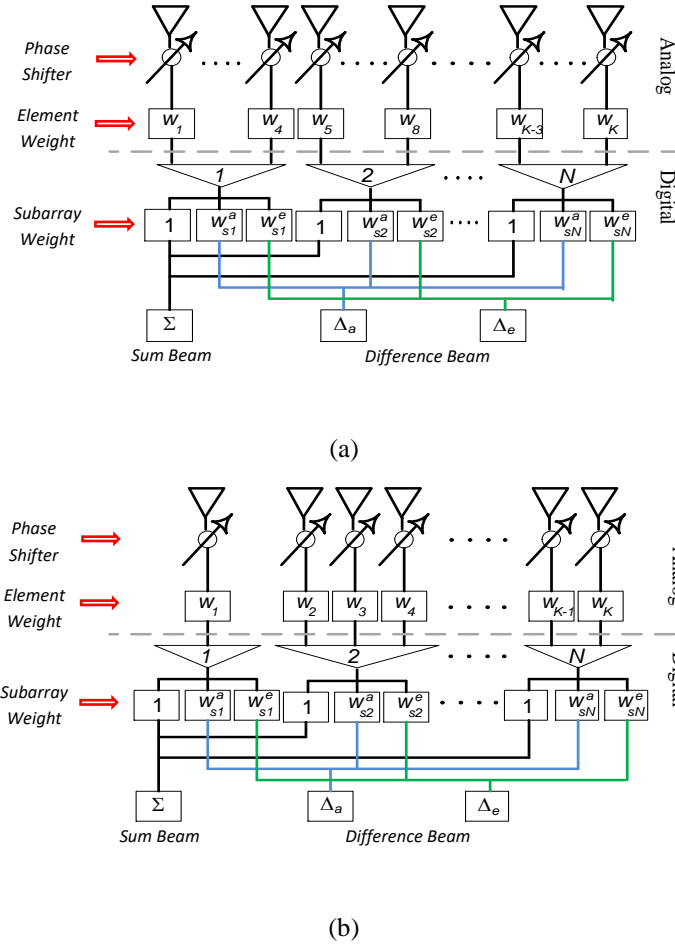
Figure 1. Illustration of subarray configuration on *K*-elements into *N*-unit non-overlapping subarrays with: (a) uniform subarrays and (b) non-uniform subarrays.

The sum pattern is optimized with fixed excitation at the element level so that $\mathbf{w}_k = \mathbf{w}_{os} = \mathbf{a}_{os}$ where $\mathbf{w}_{os}$ is the element weighting through optimization synthesis, $\mathbf{a}_{os}$ is the optimization sum vector of array factors, $u = \sin(\theta)\cos(\varphi)$, and $v = \sin(\theta)\sin(\varphi)$ [23], while the difference pattern is synthesized at the subarray level whose value is the same as the reference weight. The following are the equations for beampattern sum (Σ), beampattern difference azimuth (Δ_a), and elevation beampattern (Δ_e), respectively, i.e.,

$$\Sigma(u,v) = \mathbf{w}_k^H \mathbf{a}(u,v) \tag{3}$$

$$\Delta_a(u,v) = \mathbf{w}_{sn}^{aH} \mathbf{T}^H \mathbf{a}(u,v) \tag{4}$$

$$\Delta_e(u,v) = \mathbf{w}_{sn}^{eH} \mathbf{T}^H \mathbf{a}(u,v) \tag{5}$$

where $\mathbf{a}(u,v)$ is the steering vector in the planar array.

To synthesize a monopulse radar signal model, a detailed description is in the literature [21], [22], [27], [29] for the uniform subarray method and in the literature [23]-[26], [28] for the non- uniform subarray. Meanwhile, to clarify the beampattern on monopulse radar, it is presented in Fig. 2. Figures 2(a)-(d) show the antenna patterns of two monopulse beams where Fig. 2(a) shows two types of beams from a monopulse radar, Fig. 2(b) shows the beampattern sum results, Fig. 2(c) shows the beampattern difference, and Fig. 2(d) shows the ratio between beampattern difference to beampattern sum.

B. Existing Methods for Monopulse Radar

In this section, we discuss the methods proposed by researchers regarding monopulse subarray radar to improve radar performance, especially target tracking and monopulse ratio calculations. These methods relate to optimizing the size of subarray elements, optimizing excitation matching in subarrays, increasing maximum directivity, optimizing to obtain lower SLL to minimize the effects of interference and jamming, and computing optimization of digital processing.

1. Optimize the size of subarray elements

Several methods have been introduced in the literature to determine the size of subarrays in monopulse radar. The size of the subarray, which is actually a phased array, really determines the coherent gain on the mainlobe, SLL, and the directivity of the beam pattern, all of which determine the success of the target tracking process on the radar. There are uniform and nonuniform subarray sizes. Unlike uniform subarrays [21][22][27][29], in nonuniform subarrays each subarray in monopulse radar has an unequal number of antenna elements which generally aims to obtain a beampattern sum and difference with lower SLL and minimal excitation matching error. Various methods to obtain the optimum size for each non-uniform subarray so that the excitation matching error is minimal include: K-means clustering [23], excitation matching [24][25][28], and convex programming [26]. Still related to optimization methods, the differential evolution method is applied by [30] to regulate the size of subarrays with contiguous elements to reduce the influence of crosspoints. In digital processing which prioritizes fast and robust computing output, the steady state condition is desired as quickly as possible, so determining the size of the subarray must also take this into account.

(a)   (b)
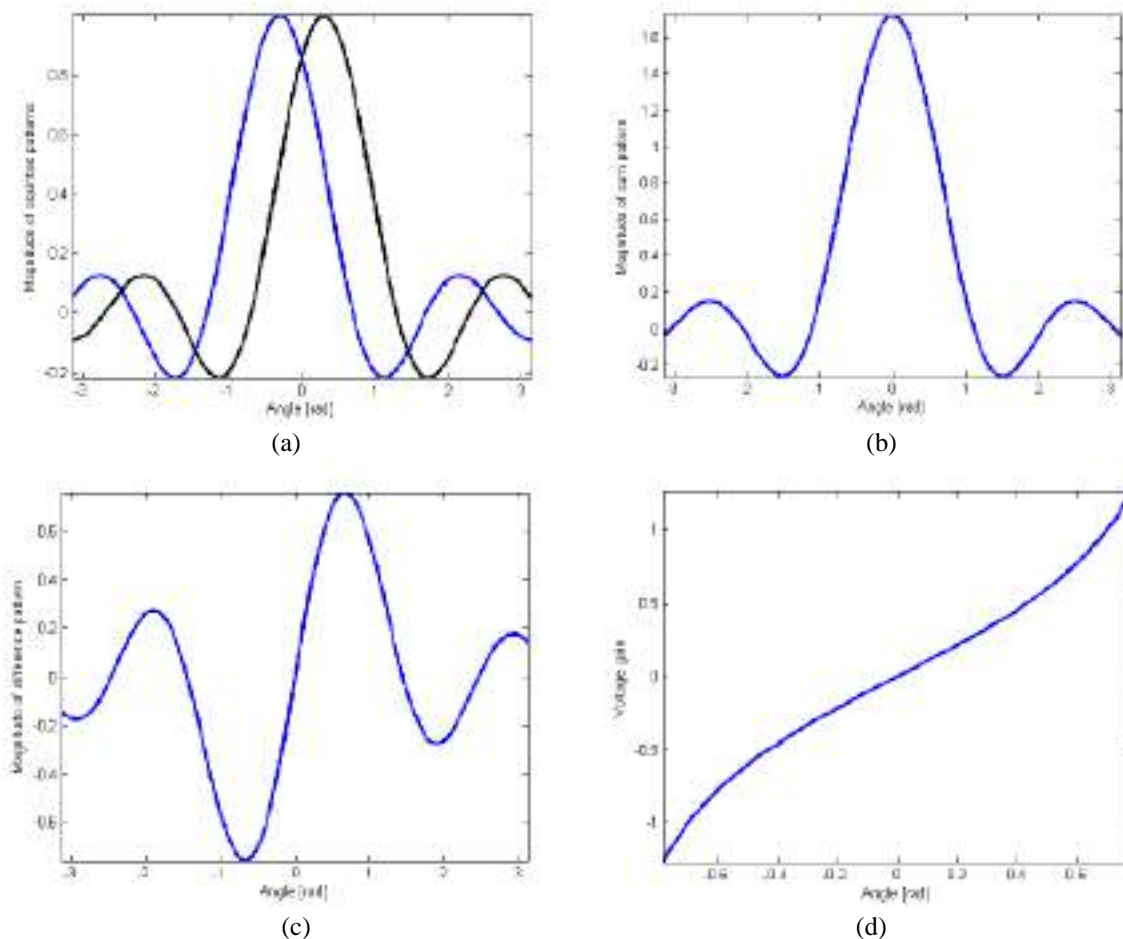
(c)   (d)

Figure 2. Beampattern on monopulse radar for: (a) two beampatterns with an angular difference of 0.3 radians, (b) beampattern from sum, (c) beampattern from difference, and (d) ratio beampattern from difference to sum.

2. Optimization of target tracking energy radiation

In monopulse radars used for target tracking, transmission power consumption must be considered. The excitation matching optimization technique is related to the energy consumption of the transmission transmitter to the target so it is necessary to consider factors such as low SLL, low component complexity, high directivity, and low cost. In optimization techniques, the size of the subarray also influences the determination of these factors, but this technique prioritizes power consumption in its computational programming capabilities. Research on the use of the excitation matching technique is by compromising between the difference pattern and the optimum sum mode obtained by a two-stage excitation matching procedure [28]. The use of subarrays with contiguous elements reported by [30] can reduce crosspoint effects on nonuniform subarrays thereby providing efficient and practical radar performance bandwidth. Meanwhile, in a study by [39] using an ultra-wideband (UWB) monopulse radar equipped with a linear frequency modulation signal, high detection and tracking resolution was obtained.

3. Optimization obtains lower SLL

There are several methods for reducing SLL in several literatures. Digital weighting in the form of Taylor for the beam sum and Bayliss taper for the difference beam is carried out at the subarray level so that the mainlobe of both beams increases [21]. In the study reported by [22] that to reduce the SLL, subarray weight selection was used using the Wiener-Hopf method, i.e., by determining the minimum square error rule on the monopulse signal output and the desired signal. Apart from getting the optimum size of each subarray so that the excitation matching error is minimal, K-means clustering also reduces SLL [23]. The K-means clustering method is a development of the excitation matching method by [24], [25], and [28] to obtain the optimum weighting and size of monopulse subarrays as well as subarray weighting with convex programming by [26]. Still related to optimization methods, the differential evolution method is applied by [30] to arrange subarrays with contiguous elements to reduce the influence of crosspoints. Apart from this, the optimization method is interesting for further research but is relatively difficult to implement. A simple method to minimize SLL while overcoming the effects of interference and jamming is adaptive beamforming in the form of moving variance distortionless response (MVDR) by [27] with a similar working principle to the study by [22]. Also, no less important was the development by [29], i.e., forming an ultra-SLL with a phase shifter control type time modulated array antenna.

Of the methods that have been developed to obtain lower SLL, they can be classified into two types, namely programming optimization methods and adaptive filtering methods. For implementation considerations, it seems that the adaptive filtering method is more relevant than the programming optimization method. The development of digital processors with high computing capabilities supports the application of this subarray optimization method.

4. Computational optimization for digital processing

Determining the subarray size clearly requires high and fast computational optimization. The consideration is to obtain a beam sum and difference in monopulse radar that has low SLL, low component complexity, high directivity, and low cost. The optimization methods developed in [23]-[26] and [28] attempt to answer these challenges, but have not yet attempted to consider transmit energy consumption and its implementation. In the study reported by [31], the implementation of FPGA with adaptive subarray or random subarray has overcome high computing requirements and resource availability.

C. Potential Strategies and Challenges in Monopulse Radar

After getting an overview of several methods used in existing monopulse radars, a scenario or strategy will be created to form a reliable subarray monopulse radar in accordance with implementation considerations. These considerations are based on various factors, i.e.: (a). simplicity of design in terms of digital processing software and hardware, (b). monopulse subarray radar design with adaptive beamforming using programming optimization, and (c). using overlapped subarrays with either equal or unequal number of elements to overcome resource limitations and involve high computing in digital processing.

Research on antennas for monopulse radar applications has been widely investigated as well as transmit/receive (T/R) modules, thus supporting the implementation of point (a). For example, in the study presented by [32], the design of a monopulse microstrip antenna array with a single layer, a working frequency of 13.85–15.1 GHz, and cheaply can provide two-dimensional target tracking performance and also supports subarray operations. Antenna design for K-band single layer with substrate integrated waveguide (SIW) for a planar array type monopulse tracking system has been reported by [33]. Another planar array antenna design with a slotted waveguide working in the Ka-band has been discussed by [34]. Meanwhile, an example of a T/R module design for monopulse radar is a study by [35] regarding a T/R module and microstrip antenna for millimeter-wave applications.

Points (b) and (c) can be a challenge and have the potential to become the latest research on monopulse radar. Point (b) has been supported by research [23]-[26], [28], and [31] how the monopulse subarray radar has subarrays that are ununiform, non-overlapped but perform satisfactorily, namely high diversity, lower SLL, and adaptive beamforming. The potential that occurs is a hybrid method of existing optimization methods or their development and the next challenge is its practical implementation. Meanwhile, point (c), which is related to monopulse overlapped subarray radar, has not yet been investigated in detail, especially with regard to the beam sum and difference calculation methods up to the monopulse ratio.

An illustration of the overlapped subarray configuration is presented in Fig. 3. However, research on radar overlapped subarrays has started with the number of elements per subarray being equal by [36] and the number of elements per subarray being unequal by [37] and [38]. In the study by [36] proposed a Phased-MIMO (PMIMO) radar approach, which is a compromise of the main advantages of PA radar, namely coherent gain, and the main advantages of MIMO radar, which produces radar performance for transmit-receive gain that outperforms two other types of radar, namely PA and MIMO. and robust against interference. Other advantages of PMIMO are increasing angular resolution, high number of detection targets, increasing identification parameters, expanding the array aperture, increasing degrees of freedom, forming virtual arrays, and robustness against beam-shape loss [36]-[38]. Thus, the challenge is to derive a signal model for the overlapped subarray and then analyze and synthesize it as done by [23]. It is possible to find a general approach or generalization of existing monopulse subarray radars.
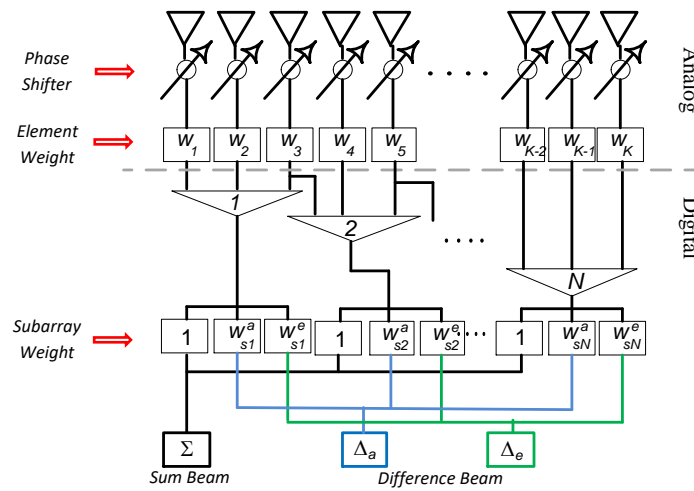
Figure 3. Illustration of the configuration of a *K*-element subarray into *N*-unit overlapped subarrays with uniform subarrays.

Table 1. Summary of Key Parameters for Monopulse Radar

Ref. No.	Types and Conditions of Arrays	Number of Targets	Key Findings
[1], [32], [39]	PA-ULA Rx	Single	Decreased monopulse angle accuracy with the CRB method, use of the DBF difference subarray, and microstrip antenna array
[2], [5], [22], [29]	PA-Planar array	Single	There are two beams, namely sum beam, difference/delta beam azimuth and delta elevation and sidelobe control is carried out on the sum beam with Taylor weighting and the delta beam with Bayliss weighting
[3], [9]	ULA	Single	Taylor and Bayliss weighting to reduce sidelobes and observe the effect of interference and jamming on the monopulse ratio and using a Doppler filter
[4]	Nonuniform planar array	Single	Overcoming grating lobe

[6], [7]	Planar array	Single	Synthesis of optimal excitation from sum and difference patterns using convex (quadratic) programming procedure to solve computational problems on large planar arrays
[8], [10]-[20]	MIMO	Multiple	Using the adaptive monopulse estimation method in mainlobe jamming and phase comparison beamforming
[21], [24], [27]	PA-subarray	Multiple	Using full digital weighting
[23], [25]-[26], [28]	Planar-subarray	Multiple	Optimization using the K-Means clustering method
[30], [31]	PA-subarray	Multiple	Optimization with DE algorithm
[33]-[35]	PA	Single	SIW method with slot antenna
[36]-[38]	PMIMO-uniform subarray	Multiple	Application of subarrays in ULA antennas

3. Conclusion

In this article we review sum-difference methods in monopulse radar. Several methods to improve the performance of monopulse radar such as subarray element size optimization, target tracking energy radiation optimization, optimization of obtaining lower SLL, and computational optimization for digital processing have been presented comprehensively. Considerations for potentially implementable monopulse radar configuration strategies are also presented. Finally, this paper aims to answer the challenge of creating a monopulse subarray radar that meets implementation requirements both in software and hardware. In the future, the author would like to investigate the implementation and explore the possibility of combining all methods from monopulse radar into a prototype form and tested for detection and tracking of single or multiple targets which also takes into account the presence or absence of noise, interference and jamming.

References

[1] R. Takahashi, K. Hirata, T. Hara, and A. Okamura, "Derivation of Monopulse Angle Accuracy for Phased Array Radar to Achieve Cramer-Rao Lower Bound," in *IEEE Int. Conf. Acoustics Speech Signal Process.*, Kyoto, Japan, Mar. 2012, pp. 2569-2572, doi: 10.1109/ICASSP.2012.6288441.

[2] K. -B. Yu, "Advanced Monopulse Processing of Phased Array Radar," in *IEEE Radar Conf.*, Arlington, VA, USA, May 2015, pp. 0174-0179, doi: 10.1109/RADAR.2015.7130991.

[3] Y. -d. He, J. Zhou and B. -h. Zhou, "Adaptive Sum and Difference Beamforming for Monopulse System with Array Antennas," in *IEEE Int. Conf. Wireless Commun. Networking Mobile Comput.*, Chengdu, China, Sept. 2010, pp. 1-5, doi: 10.1109/WICOM.2010.5600714.

[4] T. Ito, R. Takahashi and K. Hirata, "An Antenna Arrangement for Phase Comparison Monopulse DOA Estimation Using Nonuniform Planar Array," in *IEEE European Radar Conf.*, Manchester, UK, Oct. 2011, pp. 277-280.

[5] W. P. M. N. Keizer, "Element Failure Correction for A Large Monopulse Phased Array Antenna with Active Amplitude Weighting," IEEE Trans. Antennas Propag., vol. 55, no. 8, pp. 2211-2218, Aug. 2007, doi: 10.1109/TAP.2007.902008.

[6] G. Gottardi, L. Poli, P. Rocca, A. Montanari, A. Aprile, and A. Massa, "Optimal Monopulse Beamforming for Side-Looking Airborne Radars," IEEE Antennas Wireless Propag. Lett., vol. 16, pp. 1221-1224, 2017, doi: 10.1109/LAWP.2016.2628881.

[7] P. Rocca, and A. F. Morabito, "Optimal Synthesis of Reconfigurable Planar Arrays with Simplified Architectures for Monopulse Radar Applications," IEEE Trans. Antennas Propag., vol. 63, no. 3, pp. 1048-1058, Mar. 2015, doi: 10.1109/TAP.2014.2386359.

[8] Y. Yang, H. Su, J. Huang, Q. Hu, and S. Zhou, "Adaptive Monopulse Estimation in Mainlobe Jamming for Multistatic Radar," in *IEEE Radar Conference*, Oklahoma City, OK, USA, 23-27 April 2018, doi: 10.1109/RADAR.2018.8378567.

[9] Z. Li, Y. Li, and J. Zhang, "A Sidelobe Cancellation Doppler Filter for Angular Measurement in Monopulse Radar Imagination," in *3rd International Academic Exchange Conference on Science and Technology Innovation*, Guangzhou, China, 10-12 December 2021, doi: 10.1109/IAECST54258.2021.9695900.

[10] H. X. Dong, H. He, C. Q. Liang, L.Hong, J. L. Jian, G. F. Hong, Z. Xu, and J. X. Yang, "Research on Multi-Target Resolution Process with the Same Beam of Monopulse Radar," in *IEEE 17th International Conference on Communication Technology*, Chengdu, China, 27-30 October 2017, doi: 10.1109/ICCT.2017.8359805.

[11] M. F. Fernández and K. B. Yu, "Robust Adaptive Monopulse Beamforming with Low-Sidelobes," in *IEEE Radar Conference*, Boston, MA, USA, 22-26 April 2019, doi: 10.1109/RADAR.2019.8835664.

[12] T. Ito, K. Hirata, and R Takahashi, "Transmitting Phase Comparison Monopulse Estimation Using MIMO Radar Technique for Distributed Array," in *IEEE Int. Symp. Antennas Propag.*, Nagoys, Japan, Oct. 2012, pp. 78-81.

[13] C. H. An, J. Yang, R. Ran, U. Y. Pak, Y, J. Ryu, and D. K. Kim, "Enhanced Monopulse MIMO Radar Using Reliable *Aβ* Filtering," in *IEEE Military Commun.Conf.*, Orlando, FL, USA, Oct. 2012, pp. 1-6, doi: 10.1109/MILCOM.2012.6415727.

[14] S. Gogineni and A. Nehorai, "Monopulse MIMO Radar for Target Tracking," IEEE Trans. Aerospace Electron. Syst., vol. 47, no. 1, Jan. 2011, doi: 10.1109/TAES.2011.5705707.

[15] W. Rowe, J. Karlsson, and J. Li, "Error Analysis of MIMO Monopulse for Tracking Radar," in *IEEE Int. Radar Symp.*, vol. 1, Dresden, Germany, Jun. 2013, pp. 71-76.

[16] F. Belfiori, G. Babur, P. Aubry and F. L. Chevalier, "Monopulse on Transmit by Means of Orthogonal Probing Signals: Theoretical and Experimental Validations," in *Int. Radar Conf.*, Lille, France, Oct. 2014, pp. 1-4, doi: 10.1109/RADAR.2014.7060293.

[17] K. B. Yu and M. F. Fernández, "Robust Adaptive Monopulse Processing for Multiple Observations with Applications to TS-MIMO Radar," in *IEEE 11th Sensor Array and Multichannel Signal Processing Workshop*, Hangzhou, China, 08-11 June 2020, doi: 10.1109/SAM48682.2020.9104335.

[18] R. Feng, F. Uysal, and A. Yarovoy, "Target Localization Using MIMO-Monopulse: Application on 79 GHz FMCW Automotive Radar," in *15th European Radar Conference*, Madrid, Spain, 26-28 September 2018, doi: 10.23919/EuRAD.2018.8546566.

[19] K. Han and S. Hong, "MIMO Monopulse Radar for Detecting Human Targets With I/Q Curve-Length Estimations," IEEE Microwave and Wireless Components Letters, vol. 32, no. 3, pp. 214- 217, March 2022, doi: 10.1109/LMWC.2022.3142322.

[20] Z. Shafiq, C. A. Alistarh, D. E. Anagnostou, and S. K. Podilchak, "Towards MIMO-Monopulse FMCW Radar for Automotive Applications using SIW Antennas," in *9th Asia-Pacific Conference on Antennas and Propagation*, Xiamen, China, 04-07 August 2020, doi: 10.1109/APCAP50217.2020.9246063.

[21] H. Hang, D. Hongcui, and X. Ying, "Monopulse Characteristic Based on Full Digital Weighting for Phased Array Radar at Subarray Level," in *IEEE Int. Symp. Microwave Antenna Propag. EMC Technol. Wireless Commun.*, Beijing, China, Oct. 2009, pp. 693-696, doi: 10.1109/MAPE.2009.5355957.

[22] Y. Liang, "Novel Monopulse Technique Using Sidelobe Cancellation Scheme," in *IEEE Int. Conf. Wavelet Analysis Pattern Recognition*, Ningbo, China, Jul. 2017, pp. 166-170, doi: 10.1109/ICWAPR.2017.8076683.

[23] X. Yang, W. Xi, Y. Sun, T. Zeng, T. Long, and T. K. Sarkar, "Optimization of Subarray Partition for Large Planar Phased Array Radar Based on Weighted K-Means Clustering Method," IEEE J. Sel. Topics Signal Process., vol. 9, no. 8, pp. 1460-1468, Dec. 2015, doi: 10.1109/JSTSP.2015.2465306.

[24] Z. Y. Xiong, Z. H. Xu, L. Zhang, and S. P. Xiao, "Cluster Analysis for the Synthesis of Subarrayed Monopulse Antennas," IEEE Trans. Antennas Propag., vol. 62, no. 4, pp. 1738-1749, Apr. 2014, doi: 10.1109/TAP.2013.2284820.

[25] L. Manica, P. Rocca, M. Benedetti, and A. Massa, "A Fast Graph-Searching Algorithm Enabling the Efficient Synthesis of Sub-Arrayed Planar Monopulse Antennas," IEEE Trans. Antennas Propag., vol. 57, no. 3, pp. 652-663, Mar. 2009, doi: 10.1109/TAP.2009.2013423.

[26] P. Rocca, L. Manica, R. Azaro, and A. Massa, "A Hybrid Approach to the Synthesis of Subarrayed Monopulse Linear Arrays," IEEE Trans. Antennas Propag., vol. 57, no. 1, pp. 280-283, Jan. 2009, doi: 10.1109/TAP.2008.2009776.

[27] L. Y. Dai, R. F. Li, and C. Rao, "Constained Adaptive Monopulse Algorithm Based on Sub-Array," in *IET Int. Radar Conf.*, Xi'an, China, Apr. 2013, pp. 1-4, doi: 10.1049/cp.2013.0362.

[28] L. Manica, P. Rocca, and A. Massa, "Excitation Matching Procedure for Sub-Arrayed Monopulse Arrays with Maximum Directivity," IET Radar Sonar Navig., vol. 3, no. 1, pp. 42–48, 2009.

[29] M. Matsuki, K. Kihira, S. Yamaguchi, M. Otsuka, and H. Miyashita, "Sidelobe Reduction of Monopulse Patterns Using Time Modulated Array Antenna," in *IEEE Int. Symp.Phased Array Syst. Technol.*, Waltham, MA, USA, Oct. 2016, pp. 1-5, doi: 10.1109/ARRAY.2016.7832604.

[30] C. Y. Cui, Y. C. Jiao, L. Zhang, L. Lu, and H. Zhang, "Synthesis of Subarrayed Monopluse Arrays with Contiguous Elements Using a DE Algorithm," IEEE Trans. Antennas Propag., vol. 65, no. 8, pp. 4340-4345, Aug. 2017, doi: 10.1109/TAP.2017.2714021.

[31] T. Salim, M. Trinkle, R. Drake, and D. Gray, "Target Angle Estimation from Randomly Sampled Adaptive Subarray Sum and Difference Beams," in *IEEE Int. Conf. Radar*, Adelaide, SA, Australia, Sept. 2008, pp. 722-727, doi: 10.1109/RADAR.2008.4654015.

[32] H. Wang, D. G. Fang, and X. G. Chen, "A Compact Single Layer Monopulse Microstrip Antenna Array," IEEE Trans. Antennas Propag., vol. 54, no. 2, pp. 503-506, Feb. 2006, doi: 10.1109/TAP.2005.863103.

[33] B. Liu, W. Hong, Z. Kuai, X. Yin, G. Luo, J. Chen, H. Tang, and K. Wu, "Substrate Integrated Waveguide (SIW) Monopulse Slot Antenna Array," IEEE Trans. Antennas Propag., vol. 57, no. 1, pp. 275-279, Jan. 2009, doi: 10.1109/TAP.2008.2009743.

[34] T. Li, H. Meng, W. Dou, G. Xia, and H. Zhu, "Design of Low Sidelobe Slotted Waveguide Monopulse Antenna Array," in *IEEE Asia-Pacific Conf. Antennas Propag.*, Harbin, China, 2014, pp. 212-214, doi: 10.1109/APCAP.2014.6992455.

[35] Q. Xu, H. Sun, J. Yin, X. Lv, "A Millimeter Wave Variable Polarization Monopulse Frontend Based on Microstrip Array Antenna," in *IEEE Int. Conf. Microwave Technol. Comput. Electromag.*, Beijing, China, Nov. 2009, pp. 264-267, doi: 10.1049/cp.2009.1317.

[36] A. Hassanien and S. A. Vorobyov, "Phased-MIMO Radar: A Tradeoff Between Phased-Array and MIMO Radars," IEEE Trans. Signal Process., vol. 58, no. 6, pp. 3137–3151, Jun. 2010, doi: 10.1109/TSP.2010.2043976.

[37] W. Khan, I. M. Qureshi, A. Basit, and M. Zubair, "Hybrid Phased MIMO Radar with Unequal Subarrays," IEEE Antennas Wireless Propag. Lett., vol. 14, pp. 1702-1705, April 2015, doi: 10.1109/LAWP.2015.2419279.

[38] S. Tahcfulloh and G. Hendrantoro, "Phased-MIMO Radar Using Hadamard Coded Signal," in *IEEE Int. Conf. Radar Antenna Microw. Electron. Telecommun.*, Tangerang, Indonesia, Oct. 2016, pp. 13–16, doi: 10.1109/ICRAMET.2016.7849573.

[39] X. Wang, Y. Li, and B. Zou, "Detection and Tracking of Multiple Human Targets with an UWB Monopulse Radar," in *CIE International Conference on Radar*, Haikou, Hainan, China, 15-19 December 2021, doi: 10.1109/Radar53847.2021.10027929.

Biographies of Authors

Alam is an undergraduate final year student at the Department of Electrical Engineering, Universitas Borneo Tarakan, Tarakan, Indonesia. Currently he is completing his final project which focuses on signal processing for multi-antenna radar, specifically to increase target detection resolution through selection and formation of radar waveforms.

Syahfrizal Tahcfulloh received the B.Eng. degree from Universitas Gadjah Mada, Yogyakarta, Indonesia in 2003, and the M.Eng. and Ph.D. degrees from Institut Teknologi Sepuluh Nopember (ITS), Surabaya, Indonesia in 2010 and 2020, respectively, all in Electrical Engineering. Currently, he is a lecturer and associate professor with the Department of Electrical Engineering of the Universitas Borneo Tarakan, Tarakan, Indonesia. In his current position he also serves as head of the Telecommunications Systems Laboratory. His research interests include array signal processing and MIMO radar. He is a member of IEEE especially the IEEE Antennas and Propagation Society.

ANALYSIS OF THE EFFECTIVENESS OF THE FILLING MACHINE KALIX PLASTIC 501 USING THE OF OVERALL EQUIPMENT EFFECTIVENESS (OEE) METHOD AT PT. XYZ

Khusnun Widiyati[1*], Panji Pangestu[1]

[1]Department of Mechanical Engineering, Faculty of Industrial Engineering, Universitas Pertamina

Abstract

This study discusses the effectiveness of the Kalix Plastic 501 Filling machine at PT. XYZ with the Total Productive Maintenance (TPM) approach, namely by examining the Six Big Losses factors on the machine to increase the Overall Equipment Effectiveness (OEE) value. The TPM program aims to produce effectiveness in all production by participating in productive, proactive and planned activities. TPM effectiveness can be done by measuring the OEE value, where the performance of a machine can be said to be optimal if it has an OEE international standard value of > 85%. This paper provides valuable information about the performance of production machines and offers possible solutions to increase their efficiency. Based on the results of data calculations, it is known that the average value of the effectiveness of the Kalix Plastic 501 filling machine at PT. XYZ is 57,05%, meaning that this value is below the standard OEE value. Furthermore, it is known that the losses that cause low OEE values in this study are the result of deceleration loss (23%), setup and adjustment (14,78%), idle and minor stoppages (7,41%), breakdown failure (3,91%), scrap loss (0.24%), and yield loss (0%). The six losses occurred due to human factors such as lack of manpower and not following work instructions, machine factors such as sensor errors, broken filling valves, and procedural factors such as lack of PM schedules and product operations not continuing.

1. Introduction

Companies that can sell quality over quantity can have a higher value so that they dominate the market and outperform their competitors, because not all companies can produce quality products. Production plants and machinery are the main systems that play an important role in producing high-quality production, so they must always be in a reliable state. Machine reliability is very important to achieve a good production process and obtain good production results as well. Then, based on this, it can be seen how reliable the machine is, to what extent the machine can work optimally and what components in the machine can work optimally within a certain period of time.

As is the case with PT. XYZ which was established in 2000 as a company engaged in pharmaceutical manufacturing. Operating under the auspices of PT Arya Noble Group which is based on a manufacturing area or CMD. The products produced by PT. XYZ is in the form of drugs and also cosmetics. There are two goals that PT. XYZ has, namely providing satisfaction and trust in customer products that can significantly increase their business and them (customers) and provide confidence and peace of mind to customers with product quality and supply. This goal can be achieved if PT. XYZ has machines that can work optimally so that the availability and quality of products can match consumer expectations, as well as provide satisfaction and maintain customer loyalty [1].

PT. XYZ has several machines in running production, which consist of Mixing, Filling and Packaging machines. Before the process in the filling machine, there is a mixing process, namely the process of combining raw materials. The mixing process produces product materials that are ready to be packaged or called bales, later the bales are packaged with the Filling process according to the type of bales and their packaging containers. Balak or product material that is ready has three types including liquid, semisolid and solid [1].

PT. XYZ has 3 types of filling machines with similar functions but differentiated according to the form and container. The plastic kalix filling machine fills the semisolid form into a plastic container or tube. The aluminum filling machine fills the semisolid form into the aluminum packaging, while the MH filling machine fills the liquid form into the glass bottle packaging. Kalix Plastic 501 filling machine, where this machine is able to work quickly and accurately so as to reduce failure or waste of materials or products. Kalix Plastic 501 Filling Machine, as shown in Fig.1, has high accuracy so that the dose in each package has the same size and weight. This machine produces cosmetic products such as face wash, suncream, and sunblock[1].

Figure 1. Kalix Plastic 501 Filling Machine (Manual Book PT. XYZ)

The Kalix Plastic 501 Filling Machine used at PT. XYZ produces cosmetic products such as face wash, suncream, and sunblock. This machine is a special object as a material for this research because the 501 Plastic Kalix Filling machine carries out the production process every day, so this machine produces more product output, in addition to carrying out routine production processes. This machine also experiences problems that cause production targets that are not achieved every month. In addition, the request from PT. XYZ is also one of the factors that lead to the focus of research on the Kalix Plastic 501 Filling machine [1].
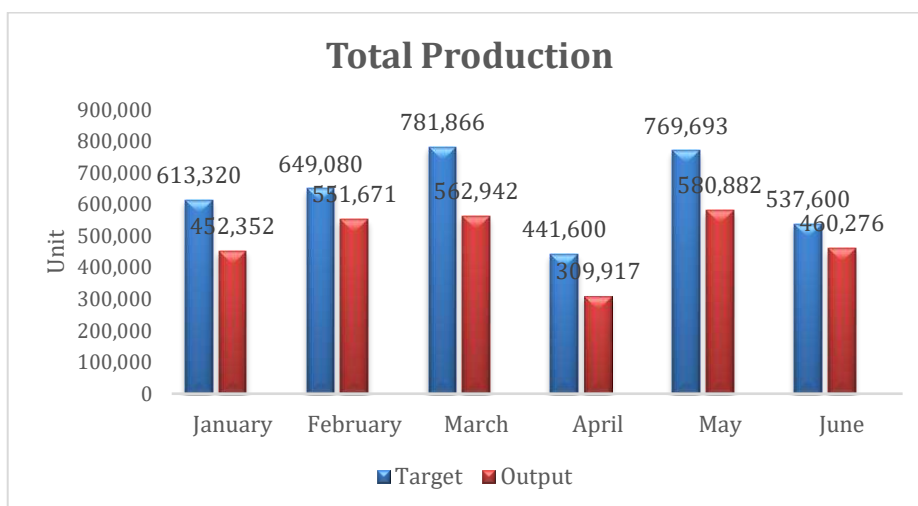

Figure 2. Graph of total production for the period January – June 2023

Based on Fig. 2, it can be observed the differences in the graphs for each month. It can be concluded that the value of the effectiveness of the Kalix 501 plastic filling machine is low, because almost every month the output

does not reach the production target. The purpose of the research is to determine the effectiveness of the Kalix 501 plastic filling machine. This research attempt to provide contribution in the field of measuring the effectiveness of Kalix 501 plastic filling machine which has never been performed before.

2. Method

A. Maintenance

Maintenance or better known as maintenance can be interpreted as activities needed to maintain or maintain the quality of equipment or machines so that they can function properly in ready-to-use conditions [2]. Companies from the lowest level to the highest level need to understand and care about the maintenance of the equipment and understand that poor maintenance can be annoying, inconvenient, wasteful, and very expensive. Good maintenance requires the need for connections between operators, machines and mechanics as well as appropriate procedures [3]. The purpose of maintenance is to return the system to its best condition so that it can function optimally, extend engine life and minimize damage. The purpose of maintenance management is to ensure the availability of devices that provide benefits, ensure the readiness of backup devices in emergency situations, maintain the safety of employees who use devices, and extend the useful life of devices [4].

B. Total Productive Maintenance (TPM)

Total Productive Maintenance (TPM) is a maintenance system that involves employees with the aim of producing effectiveness in all production with productive, proactive and planned participation and activities. So that production performance reaches the ideal of zero loss, which means zero defects, zero breakdowns, no accidents, no waste in the production process[5]. Total Productive Maintenance can be implemented through eight pillars that must be implemented by all elements within the company for successful TPM implementation.

1) *Autonomous Maintenance*
   Provide routine maintenance tasks for operators. Cleans instruments, checks instrument integrity and function, detects vibration and noise and ensures that instruments and production equipment are clean, maintained, and detects potential damage before serious damage occurs.
2) *Focused Improvement*
   Forming a work unit can be done so that it can aggressively identify instruments or work tools that are experiencing problems and provide suggestions for improvement. This pillar is preventive in reducing obstacles or losses caused by ineffective machines or equipment.
3) *Planned Maintenance*
   aims to design maintenance tasks based on the percentage of damage that has occurred or the level of damage that has been predicted, thereby reducing sudden breakdowns and providing better control over the level of component damage.
4) *Quality Maintenance*
   Discuss product quality by preventing errors during production that cause product failure and reduce the number of product defects and reduce production costs.
5) *Training & education*
   This pillar is needed to bridge the knowledge gap in implementing Total Productive Maintenance (TPM). If you don't know the tools and instruments used, it can damage the equipment and instruments, reduce labor productivity, and ultimately have a negative impact on the business.
6) *Safety Health and Environment*
   This pillar addresses companies that are responsible for three factors: safety, health, and environmental stewardship. Within this pillar, the company ensures a safe and healthy environment without any danger. For example, providing personal protective equipment to create zero accidents.
7) *TPM in Administration*
   Is administrative socialization whose aim is to ensure that all company parties have the same administrative concept. The concept is in the form of planning, purchasing, and finance in order to create a good administrative process within the company.
8) *Early Equipment Management*
   It is a pillar of TPM that uses experience from previous repair and maintenance activities to help the latest tools or instruments achieve optimal performance. The goal of this pillar is to enable the latest production instruments and systems to achieve optimal performance in the shortest possible time.

C. Overall Equipment Effectiveness (OEE)

Overall Equipment Effectiveness (OEE) is one of the measurement tools of Total Productive Maintenance (TPM) to measure and identify operational efficiency problems which will lead to actions that will improve the Company. OEE measurement is the most suitable step for semi-automatic and automated manufacturing processes. The main reason for the general application of OEE among researchers is that the OEE method is an internal but comprehensive measurement of effectiveness [6]. In particular, the measurement results are a step to make improvements so that improvement occurs.

There are 3 factors that influence the OEE value, namely, Availability loss, Performance loss, and Quality loss. This loss is the main component in measuring the OEE value on the Kalix 501 plastic filling machine. Availability loss consists of breakdown failure and setup and adjustment loss, performance loss consists of deceleration loss and idle and minor stoppages. Meanwhile, quality loss consists of scrap loss and yield loss. Basically, the OEE value is greatly influenced by the six big losses factors. Furthermore, it is known that the international standard for the OEE value is 85%, with the standard values for Availability, Performance rate, and Quality rate respectively 90%, 95%, and 99.9% [7]. To achieve optimal OEE values, it is necessary to calculate each component of these three values.

To perform the calculation of Overall Equipment Effectiveness (OEE), it is formulated as follows [8]:

$$OEE = Avaibility \times Performance\ efficiency \times Rate\ quality \qquad (1)$$

1) *Availability*

Is the ratio of active time to load time, to calculate instrument availability. The availability value is calculated using the following equation:

$$availability = \frac{Operating\ time}{Loading\ time} \times 100\% \qquad (2)$$

2) *Performance Rate*

Is a ratio that represents the capacity of equipment that produces products. To calculate the performance efficiency ratio. Performance Efficiency is calculated using a formula:

$$Performance = \frac{processed\ amount \times ideal\ cycle}{operating\ time} \times 100\% \qquad (3)$$

3) *Quality Rate*

Is a better ratio of the amount of production to the total amount of product processed. The rate of product quality can be calculated with the following equation:

$$Quality = \frac{processed\ amount - deffect\ amount}{processed\ amount} \times 100\% \qquad (4)$$

D. Six Big Losses

There are losses related to equipment within the company that are observed using the Overall Equipment Effectiveness method, which is usually referred to as the big six losses or Six Big Losses. The six major disadvantages are as follows and are divided into three types [5]:

1) *Downtime Losses*

Downtime losses are wasted time caused by production processes that cannot run due to constraints or damage to the machine [8]. The Downtime losses section consists of Breakdown losses, namely unwanted damage to factory equipment/machinery that causes losses to the company due to reduced production, time, and product rejection. Equipment failure can be classified as failure due to downtime and no operator. And Setup and adjustment, are losses caused by set up activities, including adjustments to replace the next type of product to improve the next manufacturing process. Where these two losses affect the availability value factor.

$$Breakdown\ failure = \frac{Breakdown\ time}{loading\ time} \times 100\% \qquad (5)$$

$$Set\ Up = \frac{setup\ and\ adjustment}{Laoding\ time} \times 100\% \tag{6}$$

2) *Speed Losses*

Is a situation where the process speed decreases so that it cannot meet production targets [8]. The Speed Losses section consists of Idling and minor stoppages losses. This loss can be identified from the occurance of short-term machine outages, machine stalls, and loss of machine downtime. Deceleration losses (DL) is a loss caused by the actual speed of the process which is below the optimum speed of the instrument or standard, which means that the production machine/equipment is not running optimally. Both of which affect the Performance factor.

$$idling\ and\ minor\ stoppages = \frac{non\ productive\ time}{Loading\ time} \times 100\% \tag{7}$$

$$DL = \frac{(Actual\ cycle\ time - ideal\ cycle\ time) \times produced\ amaunt}{Loading\ time} \times 100\% \tag{8}$$

3) *Quality Losses*

Are losses that occur due to products that do not comply with specifications, defective products, material losses and decreased production [9]. In the Quality losses section, it consists of Defect Losses, is a loss caused by a defective product. And Yield loss, is a loss of time and material resulting from an unstable production process, improper handling and installation of tools/machines, and operator ignorance or lack of knowledge in the production process they operate. Both of which affect the quality factor.

$$Defect\ losses = \frac{ideal\ cycle \times defect\ product}{loading\ time} \times 100\% \tag{9}$$

$$Yield\ loss = \frac{Ideal\ cylce \times scrap}{loading\ time} \times 100\% \tag{10}$$

3. Result and Discussion

In carrying out this research, data obtained from various sources such as logbooks, work order data and statements by conducting interviews with technicians and operators were used. From these data, it can be recorded to fulfill the need to know the effectiveness value of the Kalix plastic 501 filling machine. The data obtained can be seen in Tables 1-2.

Loading time, which is the machine's availability to perform operations or work, the loading time data is obtained from Available time minus Schedule loss time, Operating time data is obtained from the total length of time the machine produces a product. Schedule loss time data is scheduled maintenance on a Kalix 501 plastic filling machine, Breakdown data is data obtained when the machine experiences problems, problems, or damage during the production operation process which results in the machine shutting down and until the machine is repaired. Meanwhile, setup and adjustment data are obtained from the length of preparation time until the machine returns to production. The data in Table 1 can be used to calculate the effectiveness value of the Kalix Plastic 501 Filling machine using the Overall Equipment Effectiveness method.

Furthermore, Table 2 is data on production results produced by the Kalix Plastic 501 filling machine within a period of six months from January – June 2023. The following is the production data for the Kalix plastic 501 filling machine. Based on Table 2, it is known that the Kalix Plastic 501 Filling machine has the ideal time to produce one product within 1.5 seconds. After knowing the ideal time to produce a product, we look for the actual time that occurs in the production process to produce one product. The value of the actual time needed to produce one product is obtained from the value of the operating time divided by the value of the processed amount. Then we know the Processed amount, good product, Defect product and Scrap data from the production of the Kalix Plastic 501 Filling machine. Meanwhile, in the production process of this Kalix plastic filling machine there is no Scrap result because all products that fail can be reused, by replacing them with new containers or repack.

Table 1. Kalix Plastic Filling Machine Data

Month	Available time (sec)	Schedule Loss (sec)	Loading Time (sec)	Operating Time (sec)	Breakdown (sec)	Setup and Adj (sec)	Non–Productive time (sec)
January	1,728,000	586,800	1,141,200	919,980	43,200	167,400	10,620
February	1,987,000	637,200	1,349,200	973,620	57,600	240,300	77,680
March	2,246,000	712,800	1,533,200	1,172,800	62,000	264,600	33,800
April	1,468,800	486,000	982,800	662,400	43,200	121,500	127,440
May	2,332,800	738,000	1,594,800	1,154,540	28,800	178,200	233,260
June	1,555,200	511,200	1,044,000	806,400	54, 000	154,600	29,000

Table 2. Production data for Kalix Plastic Filling machines January – June 2023

Month	Ideal cycle time (sec)	Actual Cycle Time (sec)	Processed Amount (sec)	Good Product (sec)	Defect Product (unit)	Scrap (unit)
January	1.5	2.03	452,352	449,484	2,868	0
February	1.5	2.15	551,671	548,868	2,803	0
March	1.5	2.08	562,942	562,014	928	0
April	1.5	2.13	310,513	309,917	596	0
May	1.5	1.98	582,351	580,882	1,469	0
June	1.5	2.21	463,641	460,276	3,185	0

A. *Data Processing*

1) *Availability*

Based on the calculation results, it is known that the average availability value of the Kalix 501 plastic filling machine does not meet the standard availability value of 90%. This means that the available loading time value of the Kalix plastic 501 filling machine is not used in its entirety. It can be seen that in April the value of the loading time is the smallest compared to other months, this is because in April the joint Eid holidays are cut off. The operating time value of the Kalix Plastic 501 filling machine was obtained from the length of time the machine carried out the operation process in creating the product, but as seen in Table 3 the Kalix Plastic filling machine was not able to meet the target of available time. The average availability time is 74.38%

The occurrence of problems or breakdowns affects the operating time value which cannot work fully with the available loading time. Judging from the results, the availability value in April has a value of 67.39%, this value is lower because there is less time available due to the Eid holiday, while in other months there are obstacles or problems, namely a breakdown which makes the machine unable to meet loading times as a whole. In fact, where the problems are in the form of check weight errors, jammed nozzles and loose filling stoppers. This damage makes the operating time value low, apart from the breakdown there is also setup and adjustment which results in reduced machine availability time due to setup activities. The setup activities include installing and washing balak containers, and changing batch codes which reduce the operating time value.

Tabel 3. Availability Data January – June 2023

Month	Loading Time (sec)	Operation Time (sec)	Availability (%)
January	1,141,200	919,980	80.61%
February	1,349,200	973,620	72.16%
March	1,533,200	1,172,800	76.49%
April	982,800	662,400	67.39%
May	1,594,800	1,154,540	72.39%
June	1,044,000	806,400	77.24%
Average			74.38%

2) *Performance*

Table 4 shows the average performance value of the Kalix 501 plastic filling machine that does not meet the performance value standard of 95%, where the product produced is processed amount which takes time in the production process. The performance values in the January – June period were all below standard values, because the Kalix plastic 501 filling machine did not run at the ideal time speed. Basically, the ideal time for the Kalix

plastic 501 filling machine to create one product is 1.5 seconds, but the actual time for the Kalix plastic 501 filling machine to create one product is above the ideal time every month from January – June 2023. The difference between the actual time and The ideal time that creates the problem of low performance values for the Kalix plastic 501 filling machine, where the actual values are January (2.03 seconds), February (2.15 seconds), March (2.08 seconds), April (2.13 seconds), May (1.98 seconds) and June (2.21 seconds). The difference between the actual time and the ideal time is due to the machine experiencing a decrease in speed in the production process, which is caused by several problems such as jams in the rotary table due to the tube not fitting properly in its seat, sensors which are often active if there is a minor error causing the machine to stop, and delays in lowering container or tube because the operator is tired and not focused.

Tabel 4. Performance Data January-June 2023

Month	*Processed amount (pcs)*	*Ideal Cycle time (sec)*	*Actual Cycle Time* (sec)	*Operating time* (sec)	*Performance (%)*
January	452,352	1.5	2.03	919,980	73.75%
February	551,671	1.5	2.15	973,620	85%
March	562,942	1.5	2.08	1,172,800	71.2%
April	310,513	1.5	2.13	662,400	70.31%
May	582,351	1.5	1.98	1,154,540	75.66%
June	463,641	1.5	2.21	806,400	86.24%
Average					77.03%

3) *Quality*

Table 5 shows that the quality value produced from the Kalix 501 plastic filling machine is in accordance with the international quality value standard of 99%. These results also meet the OEE standard value because products that experience failures such as leaking products, illegible batch dates and dirty containers can still be repaired by replacing them with new containers or repacking them. A product is declared a total failure if the contents of the product are contaminated. Products that have been contaminated cannot be reused, which causes material and time losses.

Table 5. Quality Data January-June 2023

Month	Processed Amount (pcs)	Defect Product (unit)	Good Product (unit)	Quality (%)
January	452,352	2,868	449,484	99.36%
February	551,67	2,803	548,868	99.49%
March	562,942	928	562,014	99.83%
April	310,513	596	309,917	99.80%
May	582,351	1,469	580,882	99.74%
June	463,641	3,185	460,276	99.27%
Average				99.58%

4) *Overall Equipment Effectiveness (OEE)*

The OEE value on the Kalix Plastic 501 filling machine is below the standard OEE value. Where the average OEE value of the Kalix 501 plastic filling machine is 57.05%. This value is far below the standard due to the availability (74.48%) and performance (77.03%) values that are too low, due to breakdowns and high setup and adjustments which affect the availability value and the actual machine time which is different from the ideal time which causes low performance value. The OEE value of the Kalix 501 plastic filling machine can be increased by focusing on the constraints that occur in the availability and performance values. Steps to increase the availability value can focus on routine daily maintenance of machines to reduce breakdowns which result in lost production time and a new procedure is needed, namely a continuous production process, in order to reduce setup and adjustment time in cleaning, changing batch codes, and preparing logs and containers. Meanwhile, to increase the performance value by reprogramming the sensor so that when there is a minor error the sensor is not active and causes the engine to stop, paying attention to the engine rpm speed so that the engine is maintained at its ideal time, and changing the container loading dock to a horizontal shape so that the container can move smoothly without causing buildup and jamming on the rotary table. The proposal is so that the Kalix 501 plastic filling

machine can work optimally and to maintain the speed of the machine in the ideal time and maintain the quality & quantity of production. The results of the OEE calculation can be seen in Table 6.

Table 6. OEE VALUE

Month	Availability	Performance	Quality	OEE
January	80.61%	73.75%	99.36%	59.07%
February	72.16%	85%	99.49%	61.02%
March	76.49%	71.2%	99.83%	54.37%
April	67.39%	70.31%	99.80%	47.29%
May	72.39%	75.66%	99.74%	54.63%
June	77.24%	86.24%	99.27%	66.13%
Average	74.48%	77.03%	99.58%	57.05%

5) *Six Big Losses*

After knowing that the OEE value of the Kalix Plastic 501 filling machine is below the standard value, you must look for the losses that have the biggest impact on reducing the effectiveness value of the machine.

- Downtime Loss

Based on the calculation results, it is known that the largest breakdown failure value occurred in June at 5.17%. While the lowest value occurred in May of 1.8%. The breakdown loss value is affected by machines that experience problems or damage resulting in loss of production time. In May, there were 3 breakdowns where damage, obstacles or problems occurred including damaged blow and bulk nozzles, jammed nozzles and tube holders that were worn out or were no longer able to position the container perfectly. In February and March, there were high breakdown failure values, recording breakdowns 6 times, but the high loading time span did not cause high breakdown failure values like in June. These obstacles or problems cause the machine to lose time in the production process, the problems or damage occur due to the machine working fully and lack of attention to the machine components. Such as lack of attention in daily care in applying grase or grease, lack of perfect cleaning which causes some parts to become clogged. This problem causes the machine to experience damage which causes low availability values, and the machine cannot produce optimally.

Table 7 Data on the Breakdown Failure value of the Kalix Plastic 501 Filling Machine

Month	Loading Time (sec)	Breakdown Time (sec)	Breakdown Failure (%)
January	1,141,200	43,200	3.78%
February	1,349,200	57,600	4.26%
March	1,533,200	62,000	4.04%
April	982,800	43,200	4.39%
May	1,594,800	28,800	1.8%
June	1,044,000	54,000	5.17%
Average			3.91%

Furthermore, it is known that the setup and adjustment value on the Kalix 501 plastic filling machine is relatively high. This high value is caused by frequent setup activities such as washing the Filling tube, changing the batch code, and also cutting the batch. This activity becomes frequent because the Kalix 501 plastic filling machine often changes products, the Kalix 501 plastic filling machine does not work on one product continuously which causes a high setup and adjustment value. Activities carried out such as washing tubes and also changing batch codes can take as much as 45 minutes in one activity, and the lack of operators causes these activities to take a long time. On a filling machine there is only 1 operator in 1 shift where in 1 shift sometimes it can carry out setup activities 3 to 4 times, and sometimes unreadable batch codes and imperfect cutting batches require resetting and further adjustments.

Tabel 8. Setup and adjustment value data for the Kalix Plastic 501 filling machine

Month	Loading Time (sec)	Setup and Adj (sec)	Setup and adjustment loss (%)
January	1,141,200	167,400	14.66%
February	1,349,200	240,300	17.81%
March	1,533,200	264,600	17.25%
April	982,800	121,500	12.36%
May	1,594,800	178,200	11.17%
June	1,044,000	154,600	14.80%
Average			14.68%

- Speed Losses

The largest values that affect the value of idling and minor stoppages occur in April and May. The high value in April and May was due to problems with machines temporarily stopping operations which caused no production activity. Obstacles in May where the machine experienced damage problems in the form of a broken filling valve and required a replacement part, but the part had to be custom made to a company originating in France, there was an independent process which resulted in the machine not being able to produce at all until in the end the mechanic made an emergency part change by customizing using PVC. Whereas in April the constraints that caused the production process to stop temporarily, namely due to delays in the decline in logging caused by verification from the QC who were late in giving permits for the release of logs for processing of filling, so that there was no production activity on the Kalix 501 plastic filling machine until the logs were released. Apart from that, the existence of these obstacles, the checking from BPOM also made the production process temporarily stop, Table 9 below is a graph of the values of idling and minor stoppages for January – June 2023.

Table 9. Idling value data and minor stoppages

Month	Loading Time (sec)	Non–Productive Time (sec)	Idling & Minor Stoppages (%)
January	1,141,200	10,620	0.93%
February	1,349,200	77,680	5.75%
March	1,533,200	33,800	2.20%
April	982,800	127,440	12.96%
May	1,594,800	233,260	14.62%
June	1,044,000	29,000	2.77%
Average			7.41%

The value of deceleration losses is in Table 10, which shows the value of deceleration losses in the Kalix 501 plastic filling machine with a high average. The high value of deceleration losses is caused by the actual value in producing a product that is too high compared to the ideal time, where the actual value is greater and can be influenced by machines experiencing problems, problems that occur can reduce the speed of this machine. Some of these problems are the rotary table sensor which is often active, the sensor is too sensitive when an item or production container does not fit properly in its holder, and the container or tube is too late to lower due to over-tilting the container which causes the production process to experience delays. The high value of deceleration losses for this machine can be caused by the operator not paying attention to the ideal speed of this machine. Apart from this failure, the ideal speed of the machine is deliberately lowered in order to pay attention to production quality and notice if the tube is dislocated in the holder. If the machine is at its ideal speed, it will be difficult to notice failures in the production process and create obstacles in the production process.

Table 10. Deceleration losses value data

Month	Loading Time (sec)	Ideal Cycle Time (sec)	Actual Cycle Time (sec)	Processed Amount (unit)	Deceleration losses (%)
January	1,141,200	1.5	2.03	452,352	21%
February	1,349,200	1.5	2.15	551,671	26.57%
March	1,533,200	1.5	2.08	562,942	21.29%

April	982,800	1.5	2.13	310,513	19.90%
May	1,594,800	1.5	1.98	582,351	17.52%
June	1,044,000	1.5	2.21	463,641	31.53%
Average					23%

- Quality Losses

The average value of scrap losses that occur in the Kalix 501 plastic filling machine is very low, because the operator is very concerned about the production process that occurs. Apart from more observation, in the production process there is manual scanning and passing through machines, where manual scanning is done to find out whether there are leaks, dirt in the container, and also imperfect cutting batch results. Meanwhile, scanning passes through a weight checking machine to find out whether the product contents comply with standards. If a product is defective or does not meet product content tolerances, the product will be repackaged to meet product quality standards. Table 11 shows the data value of scrap losses.

Table 11. Scrap losses value data

Month	*Loading Time* (sec)	*Ideal Cycle Time* (sec)	*Defect Product* (unit)	*Scrap Losses* (%)
January	1,141,200	1.5	2,868	0.37%
February	1,349,200	1.5	2,803	0.31%
March	1,533,200	1.5	928	0.09%
April	982,800	1.5	596	0.09%
May	1,594,800	1.5	1,469	0.13%
June	1,044,000	1.5	3,185	0.45%
Average				0.24%

It is further noted that there is no yield loss value in the period January - June 2023, because products that experience failure can still be used, it's just that the container of the product is thrown away but the product contents are still reused by transferring the product contents to a new container or repacking.

Based on the 6 losses above, the deceleration loss has the highest value, namely 23%, where this loss greatly affects the decrease in the effectiveness of OEE, but if seen in Fig. 3, 80% of the problem is that there is a decrease in the effectiveness value of the Kalix 501 plastic filling machine, in addition to deceleration loss. Also, setup and adjustment loss, idle and minor stoppages, and breakdown failure. Where the four losses are the most impactful losses, for that after knowing the causes of the decrease in the value of effectiveness, repairs and maintenance must be carried out more optimally so that they can reduce the value of these losses.
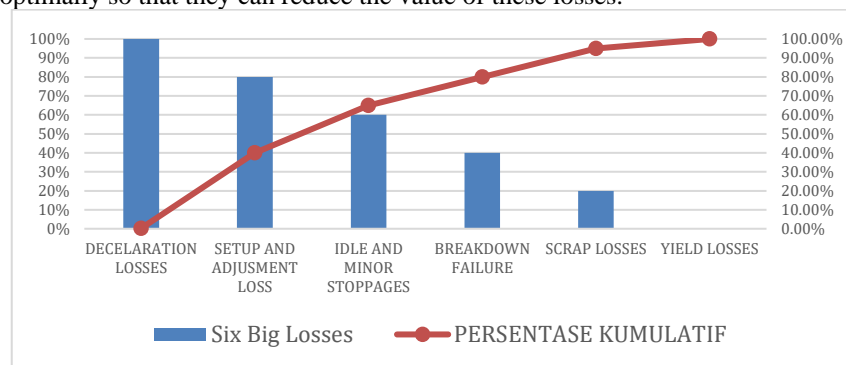

Figure 3. Pareto Charts

B. *Discussion*

Data collection was carried out over a period of 6 months starting from January – June 2023, the data was processed using equations (2.1) to (2.5) to find out the Overall Equipment Effectiveness value on the plastic kalix filling machine. Furthermore, it is known that the OEE value of the Kalix 501 plastic filling machine is below the international standard average, namely 85%. This is due to factors supporting the OEE value such as the Availability value which averages at 71.04% which is below the standard Availability value of 90% according to JIPM. The low Availability value of this machine is due to the low operating time value, the low operating time

value is due to the large amount of breakdown time and also the setup and adjustment time which is recorded in Table 1.

Apart from the Availability value which is below standard, the Performance value of this machine is also below standard. The average value over a period of 6 months, the Performance value for the Kalix 501 plastic filling machine was 69.30%, this value was far below the Performance standard, according to JIPM the Performance value standard was 95%. The low performance value of this machine is due to production results that are not optimal, which is due to the fact that the actual value of the Kalix filling machine is far different from the ideal time to create a product. Where the ideal value of the machine in creating products is 1.5 seconds but the actual value of the machine in producing products is above that value. The actual high value occurs due to the container or tube dropping late due to stacking and sensors that are too sensitive which causes the engine to stop. For the Quality value of the Kalix 501 plastic filling machine, it meets the standards where the average Quality value is 99.59%. This value is high because none of the products experienced scrap or failure that could not be reused.

Therefore, after knowing the OEE value which is below the standard average, find out the cause of the decrease in the effectiveness of the machine by using the Six Big Losses analysis to find out what losses have the most impact on the decrease in the effectiveness of the Kalix 501 plastic filling machine.

Based on the Six Big Losses analysis after knowing the OEE value below standard, it is known that there are four types of losses that affect the low effectiveness of the Kalix plastic filling machine, namely Deceleration loss 23%, Setup and Adjustment 14.78%, Breakdown Failure 3.91% and Idle and minor stoppages 7.41%. The value of the deceleration loss is due to the difference between the ideal time and the actual time in creating the product, because the machine has decreased in speed. Setup and adjustment values are affected by setup activities that are too frequent because the production process of the Kalix 501 plastic filling machine does not continue, while the idle and minor stoppages values are affected by the machine having stopped which eliminates production time. The logs were late down and the machine was damaged which required the replacement of parts, but the parts were independent, which resulted in high values of idling and minor stoppages. The breakdown loss value is caused by the machine experiencing problems and stopping the production process, where filling errors, sensor errors and broken cutting bolts cause the machine to stop.

4. Conclusion

After processing and discussing using the data obtained, after that the results of the processing are analyzed using the OEE, Six Big Losses and FTA methods. It can be concluded as follows:

1. It is known that the average effectiveness of the Kalix 501 plastic filling machine in January-June 2023 is 57.05%. Where this value is below the standard OEE value of 85% according to JIPM.
2. The looses that show the greatest influence on the lower OEE values are due to deceleration loss (23%), setup and adjustment (14.78%), idle and minor stoppages (7.41%), and breakdown failure (3.91). The difference in ideal time and the actual Kalix plastic 501 filling machine is the biggest influence and high setup activity also influences the low OEE value.

References

[1] Log Book (2010). Pharmaceuticals Genero, Perusahaan, jenis mesin, dan fungsi mesin.
[2] Sudrajat, A. (2011). *Pedoman praktis manajemen perawatan mesin industri*. Bandung: PT. Refika Aditama.
[3] Heizer., & B. Render. (2016). *Manajemen operasi, keberlangsungan dan rantai pasokan edisi 11*. Jakarta: Salemba Empat.
[4] Dewanto, I., Tony, R., & Bambang, L. (2013). Penerapan manajemen pemeliharaan dan perbaikan mesin skrap merk sacia L550-E. *Prosiding BATAN*, 449-453.
[5] Prabowo, H. A., Suprapto, Y. B., & Farida, F. (2018). The evaluation of eight pillars Total Productive Maintenance (TPM) implementation and their impact on Overall Equipment Effectiveness (OEE) and waste. *Sinergi*, 22(1), 13-18.
[6] Adam, B. A, & Sebestyen, Z. (2023). Comparison of OEE-based manufacturing productivity metrics. *Proceedings of the vreative construction conference*.
[7] Nakajima, S. (1998). *Introduction to total productive maintenance (TPM)*. Cambridge: Productivity Press Inc.
[8] Saiful, dkk. (2014). Pengukuran kinerja mesin fedekator I dengan menggunakan metode overall equipment effectiveness studi kasus pada perkebunan PT. XY. *Jemis*. 2(2), 2338-3925.

[9]   Singh, M., & Narwal, M. (2017). Measurement of overall equipment effectiveness (OEE) of a manufacturing industy: an effective lean tool. *International journal of recent trends in engineering and research.* 3(5), 268-275.

[10] Kartika, W.Y., Harsono, A., & Permata, G. (2016). Usulan perbaikan produk cacat menggunakan metode fault mode and effect analysis dan fault tree analysus pad pt.sygma examedia arkanleema. *Reka integra.* 1(4), 345-356.

[11] N.A. Wessiani., F. Yoshio. (2018). Failure Mode Effect Analysis and Fault Tree Analysis as a Combined Methodology in Risk Management. Industrial Engineering, Laboratory of Industrial Management and System Design

Biographies of Authors

Khusnun Widiyati completed her bachelor degree in Induystrial Engineering from Universitas Gadjah Mada (UGM) in 2006) with contentration in maintenance analysis. In 2010, she obtained a master degree from University Malaya, Malayisa in the field of detection of defect in ball bearing using artifical intellegence based on acoustic emission data. In 2023, she obtained doctor degree from Keio University, Japan in the field of system design engineering. She focused her research on the formulation of afective design by development of support system in drawing software.

Panji Pangestu is a student at the department of Mechanical Engineering, Universitas Pertamina.

FORECAST ANALYSIS OF FRUIT SUPPLY USING TIME-SERIES METHOD: A STUDY AT PT AEROFOOD INDONESIA

Baginda Muhammad Nasution[1], Resista Vikaliana[2*]

[1,2]Department of Logistics Engineering, Faculty of Industrial Engineering, Universitas Pertamina

Abstract

PT Aerofood Indonesia operates in the aviation logistics industry, specifically as a partner of the Garuda Indonesia airline. The main problem is the tendency to have excessive supplies of raw materials, especially when purchasing fruit because it is susceptible to damage. This phenomenon often recurs and peaks beyond dry goods capacity limits, especially the availability of papaya fruit, which often exceeds capacity by more than 50%. Therefore, this research aims to identify the optimal forecasting method for papaya fruit to overcome the problem of excessive stock. This research tested four forecasting approaches: Trend Analysis, Single Average Exponential, Double Average Exponential, and Holt's Winter Method. Forecasting calculations were carried out manually and supported by Minitab 18 software. The research showed that Holt's Winter method with a multiplicative approach produced the lowest Mean Absolute Percentage Error (MAPE), 16%. Holt's Winter method, which uses a multiplicative approach, has proven effective in producing accurate forecasts. By implementing this recommended forecasting method, it is hoped that companies can be more efficient in managing inventory and reduce the impact of losses due to excess stock.

Corresponding Author:
Resista Vikaliana
Department of Logistics Engineering,
Universitas Pertamina, Indonesia
Email:
resista.vikaliana@universitaspertamina.ac.id

1. Introduction

In the era of recovery from the COVID-19 pandemic that hit the world in 2020, many countries are starting to open their tourism doors again. The decrease in passengers results from lockdowns in several countries, including Indonesia, which has implemented PPKM (Implementation of Community Activity Restrictions) in many areas.
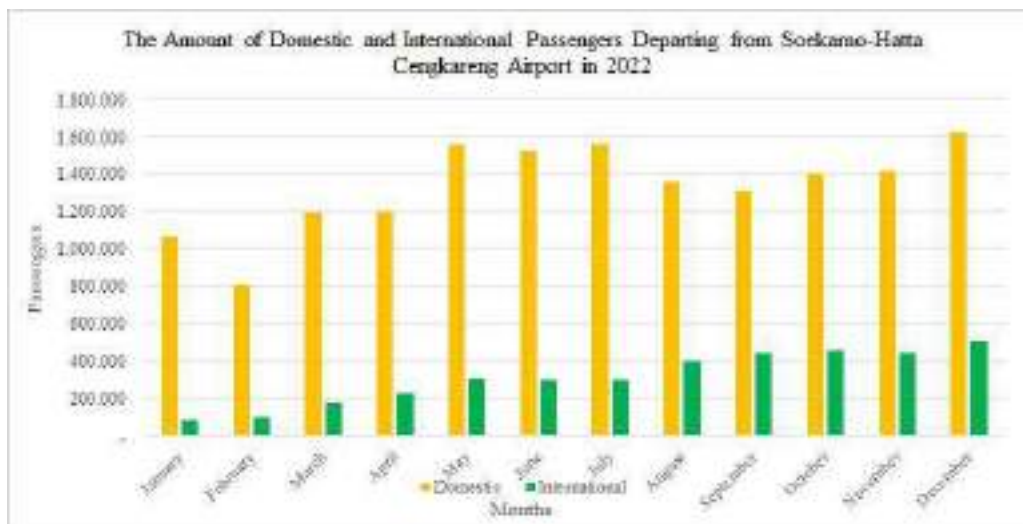
Figure 1. Data on Passenger Departures from Soekarno-Hatta in 2022 (BPS, 2022)

Based on Fig. 1 of the data above, it can be seen that the increase in domestic and international flight passengers is increasing as airlines start to increase their fleets to meet the increasing demand. PT Aerofood Indonesia, or Aerofood ACS (Aerowisata Catering Service), is a subsidiary of PT Aerowisata Group as part of the Garuda Indonesia Group subsidiary. The business led by ACS is a service company that provides services to meet aviation needs, including meeting the need for food—and cabin facilities.

The process of purchasing fruit is carried out every week, and delivery is done twice a week. Before being received, the goods will go through a quality assurance check under the specifications required by the company and then be stored in the fruit dry goods warehouse. Based on the results of informal interviews with storage supervisors, fruit often experiences an overstock phenomenon, which can result in financial losses and total capacity, and goods become unused because the shelf life for fruit is only 3 - 10 days. So, if an item is unused, it must be thrown away because it has rotted [1], [2].
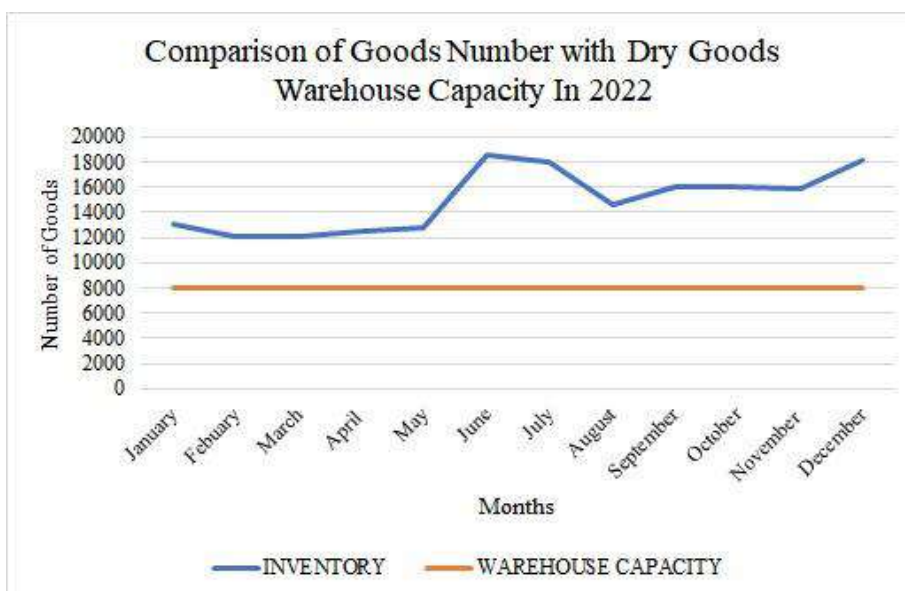

Figure 2. Comparison of Goods Number with Dry Goods Warehouse Capacity In 2022

Based on the data in Fig. 2 above, during 2022, there will always be overstock in the fruit dry goods warehouse, with an average of 50% of the total capacity in the warehouse. The fruit that often experiences

overstock is California papaya. Papaya fruit is one of the fruits that is considered an item that is often used in production.

According to [3], forecasting is a form of business that predicts future conditions by testing past conditions. Forecasting is a business function that attempts to estimate the sales use of products so that these products can be produced in a fixed quantity [4]. The forecasting or forecasting function is visible when making decisions [5]. A good decision is a decision that is based on considering what will happen when the decision is made   [6]. Forecasting is carried out to determine the number of papayas that must be ordered to meet production needs. With many overstock incidents, it is hoped that this research can provide calculations in the theoretical application by using a forecasting method that suits the need to purchase goods to prevent a surplus in the supply of papaya fruit. The Holt Winter exponential smoothing method is used when the data shows seasonal trends and patterns. This method is similar to Holt's exponential smoothing method with additional equations to handle seasonal samples [7], [8]. In this research, the objective will be to identify the appropriate type of forecasting that can be carried out when ordering papaya fruit.

2. Literature Review

Forecasting is the art or science of predicting future events. It can be done by taking historical data and predicting it for the future using some form of systematic modeling. A combination of mathematical models adapted to the manager's good judgment can be used [3], [5]. Forecasts can be classified based on the time they cover in the future. Forecasts are usually classified based on the time they cover in the future. The time horizon is divided into several categories [9], [10], namely:

1. Short-term forecasting: period of less than three months to one year. Raw material purchasing plans, work schedules, job labor and production levels.

2. Medium-term forecasting for monthly periods of up to three years. For sales, production budgeting, and cash flow planning.

3. Long-term forecasting: for three years or more. This is for planning new products, capital expenditures, location or facility development, and research and development (Research & Development). (Taylor, 2009)

Time series forecasting occurs when scientific predictions are based on time-stamped historical data, which involves establishing patterns through historical analysis and using them to observe and guide future strategic decision-making. These methods are fit if the forecasting model reference does not change much from year to year [3], [11], [12]. It is a simple method to implement and will be a good starting point for forecasting demand. Time series data is commonly used in many other fields of science, one of which is supply chain management (SCM).

1. Single Exponential Smoothing Method

    Exponential smoothing is a method that shows that the weights decrease exponentially compared to old observed values. Therefore, this method is called the exponential smoothing procedure. Like moving averages, exponential smoothing methods include single, multiple and more complex methods. They all have the same property: new values have a greater relative weight than old observed values [17].

2. Double Exponential Smoothing Method

    Brownian double exponential smoothing is a linear model proposed by Brown. In the double exponential smoothing method, smoothing is done twice. It is possible to compute double exponential smoothing with just three data values and one value for α. The logic of the Brownian double-moving average is similar to the double-moving average in that the single smoothing and double smoothing values slow down the actual data whenever there is a trend factor. The difference between single and double smoothing can be added to the single smoothing value and adjusted to Trend [17].

3. Trend Analysis Method

    Trend analysis is a statistical method that attempts to find a cause-and-effect relationship between causal or independent variables (X) and consequential variables (Y). Trend data is analyzed

and used to determine forecasts for the next period. Data migration trends can be linear, polynomial, exponential, logarithmic, or other, depending on the data sample being processed.

4.   Holt Winter Method

According to [16], if the data contains trend and seasonal components, the Holt-Winters Exponential Smoothing method can be used, which requires three smoothing parameters, namely α (for process "level") β (for trend). smoothing) and (for seasonal ingredients). According to [17], the values of α, β γ will reduce MAPE (Mean Absolute Percentage Error). There are two Holt-Winters methods, namely the additive Holt-Winters method and the multiplicative Holt-Winters method.

Predictive calculations using quantitative data usually contain data in the form of time series, where forecasting techniques often go wrong [12], [13].

1) Mean Squared Deviation(MSD)

The first measure of overall forecast error for a model is the mean squared deviation (MSD) (Heizer and Render, 2004:113). This value is calculated by adding up the absolute value of each forecast error divided by the number of data periods (n).

2) Mean Absolute Deviation(MAD)

MAD is a second way to measure the accuracy of the estimated value of the model, which is applied to the form of the average absolute error.

3) Mean Absolute Percentage Error(MAPE)

The problem with MAD and MSD is that their values depend on the expected element size. The MAD and MSD values can be significant if forecast items are measured in thousands. To avoid this problem, we can use Mean Absolute Percentage Error (MAPE). It is calculated as the average absolute difference between the predicted and actual values, expressed as a percentage of the actual value (Heizer & Render, 2004). The forecasting carried out by Ayu Ariati (2020) entitled forecasting Using the Holt-Winters Exponential Smoothing Method (Case Study: Number of Foreign Tourists Visiting Indonesia) illustrates that the research that has been carried out shows that forecasting uses the Holt's Winter method with very high data patterns. Fluctuating produces a MAPE value of 0.983%, proving that the forecasting is appropriate and very accurate. With this research, the selection of three time-series forecasting methods can be determined by the results obtained on the error values in forecasting.

3. Method

In the research that will be carried out at PT Aerofood Indonesia (ACS), the author will make observations at the company first, then determine the formulation of the problems that occur at the company, determine the objectives of the problem formulation that has been carried out and continue to collect data thoroughly to carry out In-depth analysis using the Forecasting method with the Time series method and after finding the results, the results of the research will be presented along with writing conclusions and suggestions.

This research used Ms. Excel and Minitab 18 for data analysis. Calculations in Minitab 18 will provide an overview in the form of a graph and show directly the error value in forecasting. In this research, data collection was carried out qualitatively to obtain actual data that corresponds to reality. Qualitative research aims to understand a problem in depth so that recommendations can be made following the research findings by conducting interviews with stakeholders, making field observations, and collecting actual data.

The data that will be used in this research is data on the demand for papaya fruit in 2022 for 12 months. Data is obtained to assist in calculating forecasts for demand for the next 12 months. Although daily recommendations are more specific and detailed, there are several advantages to using aggregate data [7], [8].

- Long-Term Patterns and Trends

Monthly aggregate data can help identify long-term patterns and trends that may not be visible in daily data. It can provide a deeper understanding of fluctuations in fruit supply over time.

- Easier Data Processing

Monthly aggregate data is generally easier to manage and process than daily data. It can reduce the complexity of the analysis and produce more stable recommendations.

- Noise Reduction

Daily data often tends to have more significant fluctuations or "noise" than monthly data, using aggregate data that can reduce the impact of daily fluctuations that may not represent general trends in fruit supply.

3. Result and Discussion

Based on the calculation results above, it can be concluded that the selected forecast will use the smallest MAPE value. This selected forecast is Holt Winter's with optimal values $\alpha = 0.22$, $\beta = 0.55$, and $\gamma = 0.15$ and a MAPE result of 16%.

Based on the results of the forecasting calculations above, which produce almost the same MAPE values, this indicates that the type of forecasting that has been carried out is following the criteria of the forecasting method and the data criteria used in the form of trends and seasonality which produces almost the same MAPE values and there are no significant comparisons.

The trend and seasonal data patterns are very suitable for using Holt's Winter forecasting [14], [15] in research and indeed, following the data obtained in the research conducted above, the slightest error value in forecasting is obtained with Holt's Winter method which produces a MAPE of 16 %, then in this research it can be seen that the results calculated using actual data are following theory.

The selection of the latest forecasting method is also based on the significant value of MAPE in the current forecasting carried out at PT Aerofood Indonesia with the proposed calculations in this research. The following table uses the Holt Winter Multiplicative method to compare the company's forecasted MAPE value with the forecasted MAPE value. Table 1 compares the existing forecasting at PT Aerofood Indonesia and the forecasting selected for this research.

Table 1. Comparison of existing forecasts with selected forecasts

Types of Forecasting	MAPE	Category
Existing Forecasting	59%	Not accurate
Holt's Winter Multiplicative Method	16%	Good

Based on Table 1 above, forecasting using Holt's Winter Multiplicative method is better than the company's current forecasting. This forecasting aims again to reduce the excess stock of papaya fruit. It is hoped that this forecasting method will make it easier for PT Aerofood Indonesia, a method that is more suited to the fluctuating demand for this raw material product.

After carrying out the calculations, the values obtained in Table 1 are obtained with the forecasting results using the Holt Winter method, which are results that match the data pattern obtained. The following input can be provided to the company PT Aerofood Indonesia. In the planning part of purchasing goods, it is best to enter and use the selected theory in forecasting, in this case, using the Time-series method with four selected methods. The method obtained is Holt's Winter. Companies can use a calculation base obtained from historical data as a reference and consider seasonal times such as school holidays, Hajj / Umrah, religious days, and others. Also, with the increasing growth of airline passengers in Indonesia and the end of the COVID-19 pandemic, it is hoped that this will provide an indirect picture of the pattern of goods ordered. For example, making an application that makes forecasting easier can help workers calculate how many items should be ordered with a small expected margin of error, whereas, as a company, there has been no progress in using and utilizing application technology as a whole. The contribution to this research is in terms of the forecasting calculations carried out that several things can be changed in forecasting goods without having

to make significant investments on the company's part and provide convenience for workers, saving and disposing of unnecessary funds.

4. Conclusion

Research was carried out using the time series forecasting method (Time Series) to find the most optimal forecasting for papaya fruit. Forecasting will use four methods: trend analysis, single exponential smoothing, double exponential smoothing, and Holt Winter. The research uses data on the demand for papaya fruit during 2022, calculations by Ms. Excel, and Minitab 18 software. After carrying out the calculations, it can be seen that the smallest MAPE value is 16%, then the forecasting chosen uses the Holt Winter Multiplicative method with optimal values $\alpha = 0.22$, $\beta = 0.55$, and $\gamma = 0$, 15. So, forecasting papaya fruit at PT Aerofood Indonesia is recommended using the selected method, namely Holt Winter Multiplicative.

Several suggestions will be given for further research. First, this research is still relatively small because the data was processed for only 12 months, is still short-term, and can still be further developed in forecasting calculations with other items. There is still a gap between the results of manual calculations using Minitab 18 software. Second, this research can be developed into other goods, including how many necessities such as meat, vegetables and essential goods are needed for airplane logistics.

References

[1] M. Canavari, R. Centonze, M. Hingley, and R. Spadoni, "Traceability as part of competitive strategy in the fruit supply chain," *British Food Journal*, vol. 112, no. 2, pp. 171–186, 2010, doi: 10.1108/00070701011018851.

[2] R. Zhang and J. Long, "Study on Drying Uniformity of Static Small-sized Drying Box for Fruits and Vegetables," *Procedia Eng*, vol. 205, pp. 2615–2622, 2017, doi: 10.1016/j.proeng.2017.10.201.

[3] D. Mircetic, B. R. Tabar, S. Nikolicic, and M. Maslaric, *Forecasting hierarchical time series in supply chains: an empirical investigation*. 2021. doi: 10.1080/00207543.2021.1896817.

[4] V. Gaspersz, *Total Quality Management*. Jakarta, Indonesia: PT Gramedia Pustaka Utama, 2008.

[5] K. Nikolopoulos, S. Punia, A. Schäfers, C. Tsinopoulos, and C. Chrysovalantis VasilakisVasilakis, "Forecasting and planning during a pandemic: COVID-19 growth rates, supply chain disruptions, and governmental decisions," *Eur J Oper Res*, 2020, doi: 10.1016/j.ejor.2020.08.001.

[6] V. Vlckova, F. Exnar, and O. Machac, "Quantitative Methods for Support of Managerial Decision-Making in Logistics," no. July, pp. 1015–1022, 2012, doi: 10.3846/bm.2012.130.

[7] C. D. Lewis, "Industrial and business forecasting methods," Borough Green, Sevenoaks, Kent: Butterworth, London, 1982, p. 144.

[8] M. M. Ali, M. Z. Babai, J. E. Boylan, and A. A. Syntetos, "Supply chain forecasting when information is not shared," *Eur J Oper Res*, vol. 260, no. 3, pp. 984–994, Aug. 2017, doi: 10.1016/j.ejor.2016.11.046.

[9] J. Heizer, B. Render, and C. Munsn, *Operation Management: Sustainability and Supply Chain Management*, 12th ed. Harlow, Essex, England: Pearson Education Limited, 2017.

[10] J. Heizer and B. Render, *Manajemen Operasi*, 11th ed. Salemba Empat, 2016.

[11] S. Chopra and M. S. Sodhi, "Managing risk to avoid supply-chain breakdown," *MIT Sloan Manag Rev*, vol. 46, pp. 53–61, 2004, doi: 10.1108/IJOPM-10-2012-0449.

[12] S. Sisca *et al.*, *Manajemen Operasional*. Bandung, Indonesia: Widina Bhakti Persada, 2020. [Online]. Available:
https://scholar.google.com/citations?hl=id&user=VWBjbtgAAAAJ&view_op=list_works&authuser=1&sortby=pubdate#d=gs_md_cita-d&u=%2Fcitations%3Fview_op%3Dview_citation%26hl%3Did%26user%3DVWBjbtgAAAAJ%26sortby%3Dpubdate%26authuser%3D1%26citation_for_view%3DVWBjb

[13] S. Assauri, *Manajemen Operasi Produksi (Pencapaian Sasaran. Organisasi Berkesinambungan)*, 3rd ed. Jakarta, Indonesia: PT Raja Grafindo. Persada, 2016.

[14] M. D. Reckase, *Statistics for Social and Behavioral Sciences*. 2009.

[15] A. L. Kusumatrisna *et al.*, *Statistik E-Commerce 2021*. 2021.

[16] D. Rosadi, N, W, Kurniawan. Analisis ekonometrika dan runtun waktu terapan dengan R : aplikasi untuk bidang ekonomi, bisnis, dan keuangan. Yogyakarta: Andi. 2011.

[17] S. Makridakis, S.C. Wheelwright, V.E. McGree. Metode dan Aplikasi Peramalan Jilid 1 (Terjemahan). (U. S. Andriyanto, & A. Basith, Trans.) Jakarta: Erlangga. 1999

Biographies of Authors

Baginda Muhammad Nasution is a graduate of Logistics Engineering, Universitas Pertamina in Jakarta, Indonesia. Currently, he is working as Logistic Project Coordinator at PT. Gapura Fajar Langgeng, Jakarta, Indonesia.

Resista Vikaliana is a lecturer of Logistics Engineering Departement, Faculty of Industrial Technology at Universitas Pertamina Jakarta. Her research interests include operation management, global supply chain, traceability, and halal logistics.

MONITORING CO₂ AND SO₂ EXHAUST GAS EMISSIONS ON TANKER SHIPS WITH AN IOT-BASED PLC CONTROLLER

Iqbal Nur Fajar [1], Soni Prayogi[1*]
[1]Department of Electrical Engineering, Faculty of Industrial Engineering, Universitas Pertamina

Abstract

The increasing focus on environmental sustainability has necessitated the implementation of advanced technologies for monitoring exhaust gas emissions in maritime operations. This study presents the development and application of an IoT-based Programmable Logic Controller (PLC) system for monitoring CO_2 and SO_2 emissions on tanker ships. The proposed system integrates sensors, a PLC, and wireless communication modules to continuously measure and report emission levels. The sensors detect concentrations of $CO2$ and $SO2$ in the exhaust gases, transmitting real-time data to the PLC. The PLC processes this data, which is then relayed via IoT networks to a centralized monitoring station. This setup allows for timely detection of emission levels exceeding regulatory limits, facilitating prompt corrective actions. Field trials conducted on several tanker ships demonstrated the system's reliability and accuracy in harsh maritime environments. The implementation of this IoT-based monitoring solution not only ensures compliance with international maritime emission standards but also enhances the operational efficiency of the vessels by providing actionable insights into engine performance and fuel consumption. The study concludes that the integration of IoT and PLC technologies offers a robust, scalable, and cost-effective approach to environmental monitoring in the maritime industry, promoting sustainable shipping practices.

1. Introduction

The shipping industry is one of the main sectors that influences greenhouse gas emissions globally [1]. In this context, CO_2 (*carbon dioxide*), [2] and SO_2 (*sulfur dioxide*) exhaust emissions from tankers are an important concern because of their impact on the marine and air environment [3]. These gas emissions can contribute to global climate change and air pollution which endangers human health and ecosystems [4]. Therefore, monitoring and controlling exhaust gas emissions on tankers is crucial in efforts to maintain environmental sustainability and comply with international regulations related to environmental protection [5].

In recent years, the use of *Internet of Things* (IoT) technology has grown rapidly in various industrial sectors [6], including shipping [7]. The combination of IoT with a PLC (*Programmable Logic Controller*) controller opens up new opportunities in monitoring and controlling exhaust emissions on tankers [8]. PLC controllers can efficiently integrate monitoring systems and provide fast responses to data obtained from sensors installed on ships [9]. By utilizing Internet connectivity, the collected data can be accessed in real-time remotely [10], enabling engineers and ship operators to carry out analysis and corrective action more quickly and effectively [11].

Although there have been previous efforts to reduce exhaust emissions on ships, further research is still needed to improve the efficiency and effectiveness of monitoring and control systems [12]. There are technical challenges in integrating an IoT-based PLC controller system with existing ship infrastructure and ensuring its operational reliability and safety in harsh maritime environments [13]. In addition, regulatory aspects and compliance with environmental standards also need to be considered in the development of these new solutions [14]. Therefore,

this research aims to investigate the potential for using IoT-based PLC controllers in monitoring and controlling CO_2 and SO_2 exhaust emissions on tankers, taking into account relevant technical [15], environmental [16], and regulatory aspects [17]. It is hoped that the results of this research can make a significant contribution to efforts to maintain environmental sustainability and develop environmentally friendly technology in the shipping industry.

2. Method

This research adopts an experimental approach to investigate the use of IoT-based PLC controllers in monitoring and controlling CO_2 and SO_2 exhaust emissions on tankers. First of all, planning and technical preparations are carried out for field testing. Figure 1 shows the block diagram of the system being built. The system developed consists of three main parts, namely a PLC-based machine condition monitoring system, a Raspberry Pi-based data recording system, and a warning system. This involves selecting the tanker that will be used as the research object, as well as identifying and installing the gas sensors needed to measure CO_2 and SO_2 emissions [18]. The sensors will be connected to the PLC controller system via a wired or wireless connection, depending on the configuration chosen. In addition, the IoT network infrastructure will also be prepared to enable real-time data collection and sending information to a centralized monitoring platform.
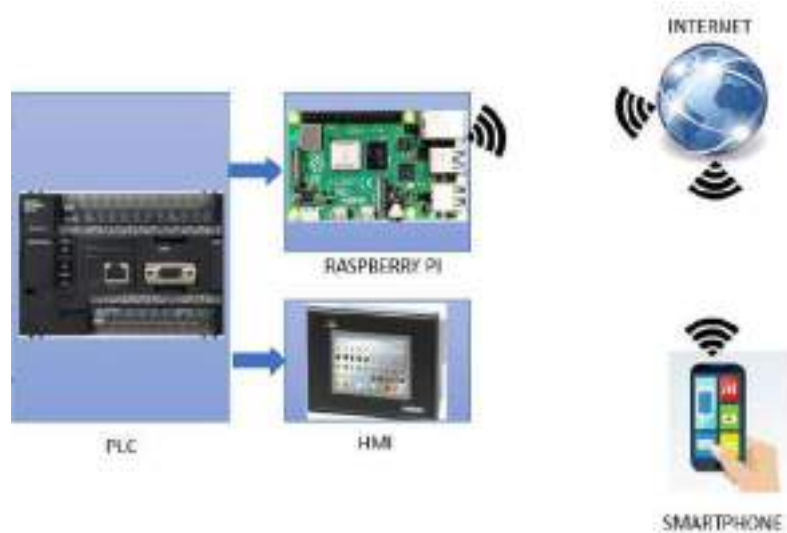
Figure 1. Block diagram of the system being built

Next, field testing was carried out to evaluate the performance of the system in monitoring and controlling exhaust gas emissions on tankers. Testing will be carried out under a variety of operational conditions representative of real situations at sea, including varying speeds and engine loads. Data collected during testing will be analyzed quantitatively to evaluate the level of accuracy and reliability of the system in detecting and measuring CO_2 and SO_2 emissions [19]. In addition, the system's response to changes in operational conditions and the effectiveness of control over gas emissions will be evaluated to determine the effectiveness of the proposed solution [20]. Test results will be used to evaluate system performance and identify potential improvements or improvements that can be made for further development.

3. Result and Discussion

Field testing of the CO_2 and SO_2 exhaust emissions monitoring system on tankers with an IoT-based PLC controller produced very valuable data for further analysis. The measurement results show that the system developed is capable of detecting and measuring CO_2 and SO_2 emission concentrations accurately in various ship operational conditions. Data obtained from the gas sensor shows variations in emissions based on engine speed and load. At low speeds and light loads, CO_2 and SO_2 emissions are relatively low, but increase significantly as engine speed and load increase. This pattern is consistent with theoretical predictions of exhaust emissions, which increase with increasing fuel consumption and engine activity.

Figure 2. Internal components of a switch cabinet installed on a container ship

The effectiveness of the control system in reducing gas emissions was also tested extensively. The IoT-based PLC controller implemented in this system exhibits high adaptive capabilities, responding to gas emission data in real time to optimize engine and exhaust system operations as seen in Figure 2. Through a specially designed control algorithm, the system can adjust engine operating parameters to reduce gas emissions [21]. In this test, the system succeeded in reducing CO_2 and SO_2 emissions by up to 20-30% under certain operational conditions compared to conditions without a controller [22]. This shows that the integration of a PLC controller with IoT not only improves monitoring but also effectiveness in controlling exhaust emissions.

In addition to technical effectiveness, practical aspects of the implementation of this system are also analyzed. One of the main challenges faced is the integration of gas sensors and PLC controllers with existing ship infrastructure. Gas sensors must be placed in strategic locations to obtain accurate data without disrupting ship operations [23]. Additionally, IoT connectivity must be stable to ensure data can be transmitted and analyzed in real time [24]. Testing shows that with proper planning and placement, these challenges can be overcome, although they require adjustments to some components of the ship's infrastructure as seen in Fig. 3. The system's reliability in various maritime environmental conditions was also tested, showing that it can withstand harsh conditions such as high humidity, vibration, and extreme temperatures.

Figure 3. Container ship with approximate location of installed SO2 sensors

From an environmental and regulatory perspective, the results of this research are very relevant. The developed monitoring and control system meets emission standards set by various international maritime regulatory bodies, such as the *International Maritime Organization* (IMO). By reducing CO_2 and SO_2 emissions, this system not only helps shipping companies comply with environmental regulations but also contributes to global efforts to reduce air pollution and the impact of climate change. In addition, the application of this technology can provide economic incentives for shipping companies through fuel savings and the potential to reduce long-term operational costs [25]. Overall, this research proves that IoT-based PLC controllers are an effective and efficient solution for monitoring and controlling exhaust emissions on tankers, paving the way for further innovation in sustainable maritime technology.

4. Conclusion

In summary, this research has proven that the CO_2 and SO_2 exhaust emissions monitoring system on tankers using an IoT-based PLC controller is an effective and efficient solution. This system successfully detects and measures gas emission concentrations with high accuracy in various ship operational conditions, and shows significant adaptive capabilities through real-time control to reduce gas emissions. Test results show a reduction in CO_2 and SO_2 emissions of up to 20-30%, which not only helps shipping companies comply with international environmental regulations, but also contributes to global efforts to reduce air pollution and the impact of climate change. Technical challenges, such as sensor integration and ship infrastructure, as well as system reliability in harsh maritime conditions, can be overcome with proper planning and adjustments. In addition to providing environmental benefits, these systems also offer the potential for economic savings through reduced fuel consumption and long-term operational costs. Overall, this research paves the way for further developments in sustainable maritime technology, supporting the shipping industry to become more environmentally friendly and efficient.

Acknowledgment

References

[1] L. Zheng, Ed., "Copyright," in *Oxy-Fuel Combustion for Power Generation and Carbon Dioxide (CO2) Capture*, in Woodhead Publishing Series in Energy. , Woodhead Publishing, 2011, p. iv. doi: 10.1016/B978-1-84569-671-9.50017-X.

[2] S. Ghufron and S. Prayogi, "Cooling System in Machine Operation at Gas Engine Power Plant at PT Multidaya Prima Elektrindo," *Journal of Artificial Intelligence and Digital Business (RIGGS)*, vol. 1, no. 2, Art. no. 2, 2023, doi: 10.31004/riggs.v1i2.21.

[3] K. El Sheikh *et al.*, "Advances in reduction of NOx and N2O1 emission formation in an oxy-fired fluidized bed boiler," *Chinese Journal of Chemical Engineering*, vol. 27, no. 2, pp. 426–443, Feb. 2019, doi: 10.1016/j.cjche.2018.06.033.

[4] B. Jin, H. Zhao, C. Zou, and C. Zheng, "Comprehensive investigation of process characteristics for oxy-steam combustion power plants," *Energy Conversion and Management*, vol. 99, pp. 92–101, Jul. 2015, doi: 10.1016/j.enconman.2015.04.031.

[5] M. Muhammad, B. Ragadita, S. Prayogi, and S. Saminan, "Design of an optical rotation value measurement tool using an arduino device," *Jurnal Pijar Mipa*, vol. 18, no. 5, Art. no. 5, Sep. 2023, doi: 10.29303/jpm.v18i5.4811.

[6] F. Hu *et al.*, "Evaluation, development, and application of a new skeletal mechanism for fuel-NO formation under air and oxy-fuel combustion," *Fuel Processing Technology*, vol. 199, p. 106256, Mar. 2020, doi: 10.1016/j.fuproc.2019.106256.

[7] R. A. Ramadhan, G. R. Kakke, I. N. Fajar, and S. Prayogi, "Smart Trash Bin Berbasis Internet Of Things Menggunakan Suplai dari Panel Surya," *G-Tech: Jurnal Teknologi Terapan*, vol. 7, no. 3, pp. 1149–1158, Jul. 2023, doi: 10.33379/gtech.v7i3.2777.

[8] X. Liang *et al.*, "Experimental and numerical investigation on sulfur transformation in pressurized oxy-fuel combustion of pulverized coal," *Applied Energy*, vol. 253, p. 113542, Nov. 2019, doi: 10.1016/j.apenergy.2019.113542.

[9] X. Hu, X. Li, G. Luo, and H. Yao, "Homogeneous and heterogeneous contributions of CO2 and recycled NO to NO emission difference between air and oxy-coal combustion," *Fuel*, vol. 163, pp. 1–7, Jan. 2016, doi: 10.1016/j.fuel.2015.09.030.

[10] S. Li, Y. Xu, and Q. Gao, "Measurements and modelling of oxy-fuel coal combustion," *Proceedings of the Combustion Institute*, vol. 37, no. 3, pp. 2643–2661, Jan. 2019, doi: 10.1016/j.proci.2018.08.054.

[11] A. P. M. Erlangga, K. S. K. Dinatha, F. E. Nainggolan, and S. Prayogi, "Prototipe Otomatisasi dan Pemantauan Sistem Hidroponik Berbasis IoT dengan Pemanfaatan Solar Panel Sebagai Sumber Energi," *G-Tech: Jurnal Teknologi Terapan*, vol. 7, no. 4, pp. 1367–1377, Oct. 2023, doi: 10.33379/gtech.v7i4.3143.

[12] M. de las Obras-Loscertales *et al.*, "NO and N2O emissions in oxy-fuel combustion of coal in a bubbling fluidized bed combustor," *Fuel*, vol. 150, pp. 146–153, Jun. 2015, doi: 10.1016/j.fuel.2015.02.023.

[13] Q. Liu, W. Zhong, and A. Yu, "Oxy-fuel combustion behaviors in a fluidized bed: A combined experimental and numerical study," *Powder Technology*, vol. 349, pp. 40–51, May 2019, doi: 10.1016/j.powtec.2019.03.035.

[14] L. Chen, S. Z. Yong, and A. F. Ghoniem, "Oxy-fuel combustion of pulverized coal: Characterization, fundamentals, stabilization and CFD modeling," *Progress in Energy and Combustion Science*, vol. 38, no. 2, pp. 156–214, Apr. 2012, doi: 10.1016/j.pecs.2011.09.003.

[15] H. Zebian and A. Mitsos, "Pressurized OCC (oxy-coal combustion) process ideally flexible to the thermal load," *Energy*, vol. 73, pp. 416–429, Aug. 2014, doi: 10.1016/j.energy.2014.06.031.

[16] G. Coraggio, L. Tognotti, D. Cumbo, N. Rossi, and J. Brunetti, "Retrofitting oxy-fuel technology in a semi-industrial plant: Flame characteristics and NOx production from a low NOx burner fed with natural gas," *Proceedings of the Combustion Institute*, vol. 33, no. 2, pp. 3423–3430, Jan. 2011, doi: 10.1016/j.proci.2010.07.024.

[17] S. Li, W. Li, M. Xu, X. Wang, H. Li, and Q. Lu, "The experimental study on nitrogen oxides and SO2 emission for oxy-fuel circulation fluidized bed combustion with high oxygen concentration," *Fuel*, vol. 146, pp. 81–87, Apr. 2015, doi: 10.1016/j.fuel.2014.12.089.

[18] F. Silviana and S. Prayogi, "Utilization of Smartphones in Experiments of Measurement of Electron-Mass Charge Ratio," *International Journal of Engineering and Science Applications*, vol. 10, no. 1, Art. no. 1, May 2023.

[19] F. Silviana and S. Prayogi, "An Easy-to-Use Magnetic Dynamometer for Teaching Newton's Third Law," *Jurnal Pendidikan Fisika dan Teknologi*, vol. 9, no. 1, Art. no. 1, Jun. 2023, doi: 10.29303/jpft.v9i1.4810.

[20] M. Marzuki, S. Prayogi, and M. Abdillah, "Data-Driven Based Model For Predictive Maintenance Applications In Industrial System," presented at the Proceedings of the International Conference on Sustainable Engineering, Infrastructure and Development, ICO-SEID 2022, 23-24 November 2022, Jakarta, Indonesia, Dec. 2023. Accessed: Jun. 04, 2024. [Online]. Available: https://eudl.eu/doi/10.4108/eai.23-11-2022.2341596

[21] S. Prayogi, Y. Cahyono, I. Iqballudin, M. Stchakovsky, and D. Darminto, "The effect of adding an active layer to the structure of a-Si: H solar cells on the efficiency using RF-PECVD," *J Mater Sci: Mater Electron*, vol. 32, no. 6, pp. 7609–7618, Mar. 2021, doi: 10.1007/s10854-021-05477-6.

[22] S. Prayogi, A. Ayunis, Y. Cahyono, and D. Darminto, "N-type H2-doped amorphous silicon layer for solar-cell application," *Mater Renew Sustain Energy*, Apr. 2023, doi: 10.1007/s40243-023-00232-9.

[23] D. Hamdani, S. Prayogi, Y. Cahyono, G. Yudoyono, and D. Darminto, "The influences of the front work function and intrinsic bilayer (i1, i2) on p-i-n based amorphous silicon solar cell's performances: A numerical study," *Cogent Engineering*, vol. 9, no. 1, p. 2110726, Dec. 2022, doi: 10.1080/23311916.2022.2110726.

[24] S. Prayogi and M. I. Marzuki, "The Effect of Addition of SnO2 Doping on The Electronic Structure of TiO2 Thin Film as Photo-Anode in DSSC Applications," *Journal of Emerging Supply Chain, Clean Energy, and Process Engineering*, vol. 1, no. 1, Art. no. 1, Sep. 2022, doi: 10.57102/jescee.v1i1.3.

[25] Z. Zainuddin, M. Syukri, S. Prayogi, and S. Luthfia, "Implementation of Engineering Everywhere in Physics LKPD Based on STEM Approach to Improve Science Process Skills," *Jurnal Pendidikan Sains Indonesia (Indonesian Journal of Science Education)*, vol. 10, no. 2, Art. no. 2, Apr. 2022, doi: 10.24815/jpsi.v10i2.23130.

Biographies of Authors

Iqbal Nur Fajar is a student of the Electrical Engineering Study Program, Faculty of Industrial Engineering, Pertamina University class of 2019. He can be contacted at email: Iqbal89@gmail.com.

Dr. Soni Prayogi, M.Si currently works in Electrical Engineering, at Pertamina University, Indonesia. He does research in materials science, condensed matter physics, magnetic compounds, and nano-/2D-materials. He can be contacted at email: soni.prayogi@ universitaspertamina.ac.id.

TECHNICAL ANALYSIS OF THE USE OF SHORE CONNECTION SERVICES AT TANKER DOCKS

Malvin Zapata [1], Soni Prayogi[1*]
[1]Department of Electrical Engineering, Faculty of Industrial Engineering, Universitas Pertamina

Abstract

The implementation of shore connection services at tanker docks is a critical advancement towards reducing the environmental impact of maritime operations. This technical analysis evaluates the effectiveness, efficiency, and economic implications of using shore power connections for tankers during docking periods. The study involves a comprehensive assessment of the infrastructure requirements, installation processes, and operational protocols associated with shore connection services. By utilizing shore power, tankers can shut down their auxiliary engines while docked, significantly reducing emissions of CO2, NOx, and particulate matter. Data collected from multiple tanker docks equipped with shore connection systems reveal substantial reductions in fuel consumption and operational costs. Additionally, the analysis highlights the technical challenges encountered, such as compatibility issues between ship and port electrical systems, and proposes solutions to enhance interoperability. The economic evaluation indicates that while initial installation costs are high, the long-term benefits in terms of reduced fuel expenditure and compliance with stringent environmental regulations justify the investment. The study concludes that shore connection services represent a viable and sustainable solution for the maritime industry, promoting cleaner port environments and contributing to the global effort to mitigate climate change. Further research is recommended to optimize system designs and expand the adoption of this technology across different types of ports and vessels.

1. Introduction

In recent decades, the maritime industry has come under increasing pressure to reduce the environmental impact of ship operations [1]. One of the main issues is the greenhouse gas emissions and other air pollutants produced by ships [2], especially when docked at ports [3]. Tankers, with their large size and significant fuel consumption, are a major contributor to this [4]. The use of fossil fuel-based generators to provide electricity when ships are at dock is a source of emissions that needs to be addressed [5]. In this context, shore connection services [6], or often called cold ironing, emerge as a potential solution [7]. This technology allows ships to turn off their engines and switch to using electricity from land [8], which is usually cleaner and more efficient [9].

Implementing shore connections at tanker docks is not only about reducing emissions, but is also related to increasing operational efficiency and reducing long-term operational costs [10]. By utilizing energy sources from land [11], ships can reduce the use of expensive and inefficient fossil fuels [12], and reduce the need for engine maintenance [13]. However, the transition to a shore connection system faces various technical and economic challenges [14]. Implementation of this system requires substantial infrastructure investment at the port, as well as technical adjustments to the tanker for compatibility with the onshore electrical system [15]. In addition, international technical standards need to be widely adopted to ensure system interoperability and security.

This research aims to analyze the technical aspects of using shore connection services at tanker docks. Through a descriptive analysis approach, this research will identify optimal system configurations, evaluate integration with port infrastructure [16], and examine existing challenges and opportunities [17]. Data will be collected through field observations [18], interviews with port operators [19], and a review of relevant literature [20]. It is hoped that the research results will provide comprehensive insight into the advantages and obstacles in implementing shore connections, as well as practical recommendations for increasing the adoption of this technology [21]. Thus, this research contributes to global efforts to achieve more sustainable and environmentally friendly maritime operations.

2. Method

This research uses a qualitative descriptive approach to analyze the technical aspects of using shore connection services at tanker docks. The descriptive method was chosen because it allows researchers to observe and describe phenomena in detail, without intervention or manipulation of variables. Data was collected through several techniques, including field observations, in-depth interviews with port operators and tanker crews, and literature reviews. Field observations were carried out at several major ports that have implemented or are currently testing shore connection systems [22]. It provides a first-hand overview of the technical configurations used, challenges faced during implementation, and solutions that have been implemented as seen in Figure 1. In-depth interviews were conducted with various stakeholders, including port managers, technicians, and ship crew, to gain a comprehensive perspective on system operations and their practical experiences.
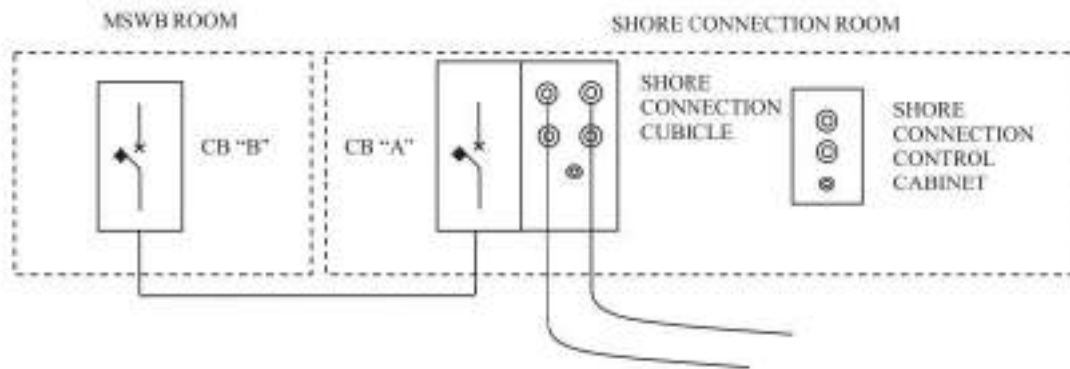

Figure 1. Simple block diagram of shore connection services at a tanker berth.

The literature review includes case studies, previous research papers, and technical documents related to shore connections. This literature is analyzed to understand the latest developments in shore connection technology, applicable international standards, and best practices that have been identified in various ports throughout the world. The data collected was then analyzed using the thematic analysis method to identify main patterns and themes related to the use of shore connections. The results of this analysis are used to develop practical recommendations that can help ports and ship operators adopt this technology more effectively [23]. This research also considers economic aspects, by analyzing the initial investment costs and long-term benefits of using shore connections, as well as the impact on reducing emissions and operational efficiency of tanker ships [24]. Thus, this research method is designed to provide a comprehensive understanding of the potential and challenges of using shore connection services, as well as their contribution to the sustainability of the maritime industry.

3. Result and Discussion

Implementation of Shore Connection at Main Ports

This research looks at the implementation of shore connections at several major ports that have adopted this technology, such as the Port of Rotterdam, the Port of Singapore, and the Port of Los Angeles. Observation results show that the technical configuration of shore connections at each port varies according to operational needs and available electricity capacity [25]. In the Port of Rotterdam, for example, the shore connection system uses high-voltage electrical connections (6.6 kV to 11 kV) which allows large tankers to meet their power needs without the need to use fossil fuel generators as seen in Figure 2. Meanwhile, the Port of Los Angeles is adopting a more flexible approach by providing low and high-voltage options, allowing vessels with varying technical specifications to use shore connection facilities.
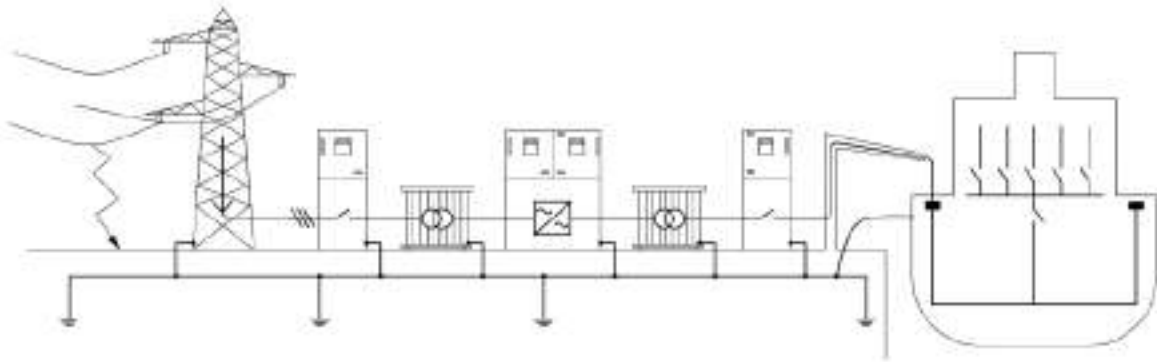
Figure 2. Port with system power supply via primary line 6.6 kV to 11 kV with single phase fault at delivery point.

Interviews with port operators and technicians revealed that one of the main challenges in implementing shore connections is technical adjustments to tankers. Older tankers often require significant modifications to their electrical systems to be compatible with shore connections. Additionally, international standardization is a critical issue, with the need to harmonize safety and operational protocols for compatibility between ports [26]. However, despite technical challenges and high initial investment, the long-term benefits derived from emissions reductions and operational efficiencies were consistently recognized by all stakeholders interviewed.

Energy Efficiency and Emission Reduction

Data from observations and interviews show that the use of shore connections significantly reduces fuel consumption and pollutant emissions from anchored tankers. For example, at the Port of Singapore, the implementation of shore connections on several large tankers has shown a reduction in fuel consumption of up to 30% during the berthing period. This reduction not only reduces operational costs, but also reduces CO_2, N_{ox}, and SOx emissions which are major contributors to air pollution and climate change [27]. A case study at the Port of Los Angeles also showed similar results, with a reduction in CO_2 emissions of up to 40% compared to ships using diesel-fueled generators during anchorage.

Economic analysis reveals that although the initial investment costs for shore connection infrastructure are quite high, the long-term savings in fuel costs and engine maintenance costs can offset this investment. For example, in the Port of Rotterdam, estimates show that the port could reach a break-even point within 5-7 years after implementing shore connections, with the potential for significant operational savings thereafter [28]. In addition, government incentives and increasingly stringent environmental regulations provide additional encouragement for ports and ship operators to adopt this technology.

Operational Challenges and Solutions

This research also identifies several operational challenges faced in implementing shore connections. One of the main challenges is the technical compatibility between ships and port infrastructure. Older tankers often require significant modifications to integrate shore connection systems, including electrical system upgrades and installation of additional equipment. This creates additional costs and operational downtime that ship operators need to take into account. In addition, differences in technical standards between countries and ports are an obstacle to wider implementation as seen in Figure 3. For example, different electrical voltages and frequencies in various ports require ships to have more flexible adaptability.
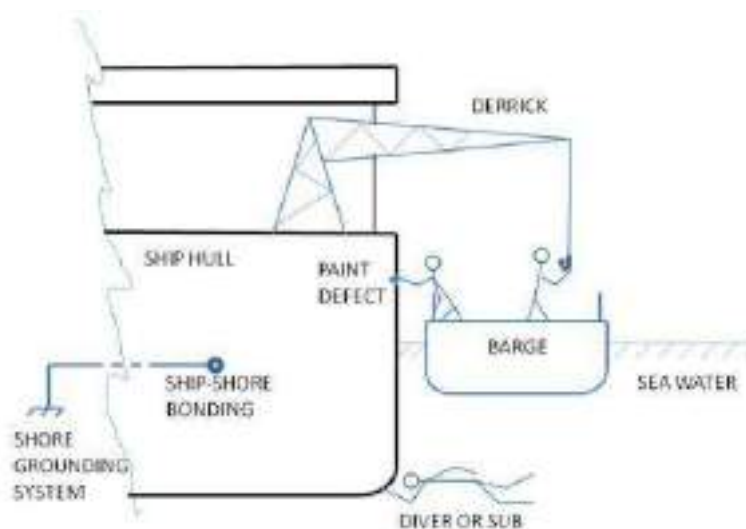
Figure 3. The dock running the Shore Connection Service at the Tanker Pier is moored alongside.

To overcome these challenges, several solutions have been identified. First, the development of international technical standards that can be applied globally is essential to ensure operational compatibility and security. The *International Maritime Organization* (IMO) and *International Electrotechnical Commission* (IEC) are working on this standardization, but implementation and widespread adoption still take time. Second, ports can offer financial incentives to ships that invest in upgrading their electrical systems. This incentive can take the form of a reduction in port fees or a direct subsidy for the installation of shore connection equipment. Third, ports and ship operators can work together on training programs to improve the technical skills of ship crew and port technicians in operating and maintaining shore connection systems.

Future Potential and Recommendations

Based on the results and analysis carried out, the use of shore connections has great potential to improve sustainability and operational efficiency in the maritime industry, especially for tankers. To maximize this potential, several strategic recommendations are proposed. First, ports must continue to invest in shore connection infrastructure and ensure the availability of this service for various types of vessels. Second, collaboration between ports, ship operators, and international regulatory bodies needs to be improved to accelerate the development and adoption of uniform technical standards [29]. Third, financial incentives and supporting regulations need to be expanded to encourage more ship operators to adopt shore connection technology [30]. Governments can play an important role in this by offering subsidies, tax breaks, or other incentives to ports and ship operators that invest in green technologies. Fourth, research and development must continue to be encouraged to increase efficiency and reduce the costs of implementing shore connections. New technologies such as automation systems and smart grids can provide innovative solutions to existing operational challenges.

By implementing these recommendations, the maritime industry can more quickly transition to cleaner and more efficient operations, making a significant contribution to reducing global emissions and protecting the marine environment. This research shows that despite technical and economic challenges, the long-term benefits of using shore connections far outweigh the initial costs, making them a worthwhile investment for a more sustainable future for the shipping industry.

4. Conclusion

In summary, this research examines the technical aspects of using shore connection services at tanker berths, with a focus on implementation, energy efficiency, emission reduction, operational challenges and potential solutions. The study results show that shore connection is an effective solution for reducing fuel consumption and pollutant emissions, as well as increasing the operational efficiency of anchored tankers. Implementation of this technology in major ports, such as Rotterdam, Singapore and Los Angeles, has proven significant environmental and economic benefits. However, challenges such as high initial investment costs, the need for technical adjustments to vessels, and differences in international standards need to be overcome. Recommendations to address these challenges include developing global technical standards, providing financial incentives, and increasing collaboration between ports, ship operators, and regulatory agencies. This research confirms that shore

connections are a worthwhile investment for a more sustainable future for the maritime industry, and with the right support, this technology can be widely adopted to achieve cleaner and more efficient shipping operations..

Acknowledgment

References

[1] H. N. Psaraftis, T. Zis, and S. Lagouvardou, "A comparative evaluation of market based measures for shipping decarbonization," *Maritime Transport Research*, vol. 2, p. 100019, Jan. 2021, doi: 10.1016/j.martra.2021.100019.

[2] D. Darminto *et al.*, "Unrevealing tunable resonant excitons and correlated plasmons and their coupling in new amorphous carbon-like for highly efficient photovoltaic devices," *Sci Rep*, vol. 13, no. 1, Art. no. 1, May 2023, doi: 10.1038/s41598-023-31552-5.

[3] D. Hamdani, S. Prayogi, Y. Cahyono, G. Yudoyono, and D. Darminto, "The influences of the front work function and intrinsic bilayer (i1, i2) on p-i-n based amorphous silicon solar cell's performances: A numerical study," *Cogent Engineering*, vol. 9, no. 1, p. 2110726, Dec. 2022, doi: 10.1080/23311916.2022.2110726.

[4] F. Ballini and R. Bozzo, "Air pollution from ships in ports: The socio-economic benefit of cold-ironing technology," *Research in Transportation Business & Management*, vol. 17, pp. 92–98, Dec. 2015, doi: 10.1016/j.rtbm.2015.10.007.

[5] J. Pruyn and J. Willeijns, "Cold ironing: modelling the interdependence of terminals and vessels in their choice of suitable systems," *Journal of Shipping and Trade*, vol. 7, no. 1, p. 17, Jul. 2022, doi: 10.1186/s41072-022-00119-4.

[6] S. Prayogi, F. Silviana, and Z. Zainuddin, "Understanding of the Experimental Concept of Radiation Absorption of Radioactive Materials," *Journal of Physics: Theories and Applications*, vol. 7, no. 1, Art. no. 1, Mar. 2023, doi: 10.20961/jphystheor-appl.v7i1.70138.

[7] E. A. Sciberras, B. Zahawi, and D. J. Atkinson, "Electrical characteristics of cold ironing energy supply for berthed ships," *Transportation Research Part D: Transport and Environment*, vol. 39, pp. 31–43, Aug. 2015, doi: 10.1016/j.trd.2015.05.007.

[8] S. Prayogi, "Thin Layer Deposition of a-Si: H n-Type Hydrogenated Amorphous Silicon using PECVD," *Journal of Science and Informatics for Society (JSIS)*, vol. 1, no. 1, Art. no. 1, Feb. 2023.

[9] S. German-Galkin and D. Tarnapowicz, "Energy Optimization of the 'Shore to Ship' System—A Universal Power System for Ships at Berth in a Port," *Sensors (Basel)*, vol. 20, no. 14, p. 3815, Jul. 2020, doi: 10.3390/s20143815.

[10] A. Innes and J. Monios, "Identifying the unique challenges of installing cold ironing at small and medium ports – The case of aberdeen," *Transportation Research Part D: Transport and Environment*, vol. 62, pp. 298–313, Jul. 2018, doi: 10.1016/j.trd.2018.02.004.

[11] D. Hamdani, S. Prayogi, Y. Cahyono, G. Yudoyono, and D. Darminto, "The Effects of Dopant Concentration on the Performances of the a-SiOx:H(p)/a-Si:H(i1)/a-Si:H(i2)/μc-Si:H(n) Heterojunction Solar Cell," *International Journal of Renewable Energy Development*, vol. 11, no. 1, pp. 173–181, Feb. 2022, doi: 10.14710/ijred.2022.40193.

[12] S. Prayogi and M. I. Marzuki, "The Effect of Addition of SnO2 Doping on The Electronic Structure of TiO2 Thin Film as Photo-Anode in DSSC Applications," *Journal of Emerging Supply Chain, Clean Energy, and Process Engineering*, vol. 1, no. 1, Art. no. 1, Sep. 2022, doi: 10.57102/jescee.v1i1.3.

[13] M. Viana *et al.*, "Impact of maritime transport emissions on coastal air quality in Europe," *Atmospheric Environment*, vol. 90, pp. 96–105, Jun. 2014, doi: 10.1016/j.atmosenv.2014.03.046.

[14] S. Prayogi, Y. Cahyono, I. Iqballudin, M. Stchakovsky, and D. Darminto, "The effect of adding an active layer to the structure of a-Si: H solar cells on the efficiency using RF-PECVD," *J Mater Sci: Mater Electron*, vol. 32, no. 6, pp. 7609–7618, Mar. 2021, doi: 10.1007/s10854-021-05477-6.

[15] S. Fang and H. Wang, "Introduction to the Multi-energy Maritime Grids," in *Optimization-Based Energy Management for Multi-energy Maritime Grids*, S. Fang and H. Wang, Eds., Singapore: Springer, 2021, pp. 1–29. doi: 10.1007/978-981-33-6734-0_1.

[16] S. Prayogi, Y. Cahyono, and D. Darminto, "Electronic structure analysis of a-Si: H p-i1-i2-n solar cells using ellipsometry spectroscopy," *Opt Quant Electron*, vol. 54, no. 11, p. 732, Sep. 2022, doi: 10.1007/s11082-022-04044-5.

[17] K. T. Gillingham and P. Huang, "Long-Run Environmental and Economic Impacts of Electrifying Waterborne Shipping in the United States," *Environ. Sci. Technol.*, vol. 54, no. 16, pp. 9824–9833, Aug. 2020, doi: 10.1021/acs.est.0c03298.

[18] Z. Zainuddin, M. Syukri, S. Prayogi, and S. Luthfia, "Implementation of Engineering Everywhere in Physics LKPD Based on STEM Approach to Improve Science Process Skills," *Jurnal Pendidikan Sains Indonesia (Indonesian Journal of Science Education)*, vol. 10, no. 2, Art. no. 2, Apr. 2022, doi: 10.24815/jpsi.v10i2.23130.

[19] S. Prayogi, A. Ayunis, Y. Cahyono, and D. Darminto, "N-type H2-doped amorphous silicon layer for solar-cell application," *Mater Renew Sustain Energy*, Apr. 2023, doi: 10.1007/s40243-023-00232-9.

[20] I. Krämer and E. Czermański, "Onshore power one option to reduce air emissions in ports," *NachhaltigkeitsManagementForum*, vol. 28, no. 1, pp. 13–20, Jun. 2020, doi: 10.1007/s00550-020-00497-y.

[21] L. Tian *et al.*, "Shipping emissions associated with increased cardiovascular hospitalizations," *Atmospheric Environment*, vol. 74, pp. 320–325, Aug. 2013, doi: 10.1016/j.atmosenv.2013.04.014.

[22] J. Qi, S. Wang, and C. Peng, "Shore power management for maritime transportation: Status and perspectives," *Maritime Transport Research*, vol. 1, p. 100004, Jan. 2020, doi: 10.1016/j.martra.2020.100004.

[23] S. Prayogi, "Enhancement of the Silicon Nanocrystals' Electronic Structure within a Silicon Carbide Matrix," *Indonesian Journal of Chemistry*, vol. 24, no. 1, Art. no. 1, Feb. 2024, doi: 10.22146/ijc.79864.

[24] R. Winkel, U. Weddige, D. Johnsen, V. Hoen, and S. Papaefthimiou, "Shore Side Electricity in Europe: Potential and environmental benefits," *Energy Policy*, vol. 88, pp. 584–593, Jan. 2016, doi: 10.1016/j.enpol.2015.07.013.

[25] B. Stolz, M. Held, G. Georges, and K. Boulouchos, "The CO2 reduction potential of shore-side electricity in Europe," *Applied Energy*, vol. 285, p. 116425, Mar. 2021, doi: 10.1016/j.apenergy.2020.116425.

[26] B. Knopf, P. Nahmmacher, and E. Schmid, "The European renewable energy target for 2030 – An impact assessment of the electricity sector," *Energy Policy*, vol. 85, pp. 50–60, Oct. 2015, doi: 10.1016/j.enpol.2015.05.010.

[27] V. Eyring *et al.*, "Transport impacts on atmosphere and climate: Shipping," *Atmospheric Environment*, vol. 44, no. 37, pp. 4735–4771, Dec. 2010, doi: 10.1016/j.atmosenv.2009.04.059.

[28] F. Silviana and S. Prayogi, "Utilization of Smartphones in Experiments of Measurement of Electron-Mass Charge Ratio," *International Journal of Engineering and Science Applications*, vol. 10, no. 1, Art. no. 1, May 2023.

[29] F. Silviana and S. Prayogi, "An Easy-to-Use Magnetic Dynamometer for Teaching Newton's Third Law," *Jurnal Pendidikan Fisika dan Teknologi*, vol. 9, no. 1, Art. no. 1, Jun. 2023, doi: 10.29303/jpft.v9i1.4810.

[30] M. Marzuki, S. Prayogi, and M. Abdillah, "Data-Driven Based Model For Predictive Maintenance Applications In Industrial System," presented at the Proceedings of the International Conference on Sustainable Engineering, Infrastructure and Development, ICO-SEID 2022, 23-24 November 2022, Jakarta, Indonesia, Dec. 2023. Accessed: Jun. 04, 2024. [Online]. Available: https://eudl.eu/doi/10.4108/eai.23-11-2022.2341596

Biographies of Authors

	Malvin Zapata 🆔 🔍 SC 📘 is a student of the Electrical Engineering Study Program, Faculty of Industrial Engineering, Pertamina University class of 2019. He can be contacted at email: Iqbal89@gmail.com.
	Dr. Soni Prayogi, M.Si 🆔 🔍 SC 📘 currently works in Electrical Engineering, at Pertamina University, Indonesia. He does research in materials science, condensed matter physics, magnetic compounds, and nano-/2D-materials. He can be contacted at email: soni.prayogi@ universitaspertamina.ac.id.

STRENGTH AND DEFORMATION ANALYSIS ON CAR DOOR DESIGN FOR ENERGY SAVING CONTEST

Sylvia Ayu Pradanawati[1], Dinny Harnavy[2], Byan Wahyu Riyandwita[1*], Apri Roni Ikhtiar[1], Dimas Wahyu Sasongko[1], Ahmad Imam Khoiruddin[1], Afif Sulthan R. N.[1], Muhammad Rusydi[1], Yafendra Arie Saputra[1], Rizky Susilo Widodo[1]

[1]Department of Mechanical Engineering, Faculty of Industrial Engineering, Universitas Pertamina
[2]Department of Mechanical Engineering, Faculty of Industrial Engineering, Institut Teknologi Sepuluh Nopember

Abstract
The car door is a vital component of an automobile, playing a key role in passenger safety during accidents. For an energy-saving competition, the strength of a car prototype's door was thoroughly examined using Finite Element Analysis (FEA). This study involved three testing methods: pole side impact, side impact, and door slam tests. Simulations were conducted using the Finite Element Method (FEM) with aluminum alloy 6061-T4, type-E fiberglass, and type-S fiberglass as materials. These materials were selected based on their stress properties, mass, and cost. The simulation indicated that the side impact test produced the highest stress levels, especially in the fiberglass materials. While the aluminum alloy exhibited higher von Mises stress than its tensile strength in one case, both types of fiberglass maintained safety as their tensile strengths exceeded the maximum von Mises stress. The pole side impact test showed aluminum's highest stress and deformation, whereas fiberglass materials showed higher stress and deformation in the side impact test. The door slam test demonstrated minimal stress and deformation across all materials. Among the three, type-E fiberglass demonstrated the most favorable and safest performance. Consequently, type-E fiberglass is highly recommended as the ideal material for the car prototype's door.

1. Introduction

With the depletion of the earth's fuel reserves, it has become imperative to devise a strategy that addresses the global fuel demand by either reducing fuel consumption or identifying alternative sources of renewable energy. In light of advancements in technology, the global automotive industry has begun manufacturing vehicles with significantly lower fuel consumption rates [1]. To equip students in Indonesia to effectively confront the energy crisis, the Ministry of Education and Culture of the Indonesian Government (Kemendikbud RI) has organized a competition titled "Kontes Mobil Hemat Energy (KMHE)" focused on energy-efficient vehicles. The objective is for students to design and construct vehicles that exhibit low fuel consumption, high safety standards, and environmental friendliness. All vehicle designs submitted must adhere to the standards and regulations set forth by the organizers, which include specifications for the car doors. The car door design must meet certain parameters, such as a minimum size of 50×80 cm, ensuring driver and passenger safety, and secure installation to the vehicle's body while allowing for easy ingress and egress within 10 seconds [2]. To ensure compliance with all the established standards, a thorough strength analysis of the designs is mandated.

The testing of car door strength has been conducted several times by researchers using different methods. Shikkerimath et al. analyzed the car door design of the TATA Indica V2 using a pole side impact mechanism at velocities of 30 m/s and 90 m/s [3]. Long et al. tested the strength of the Toyota Yaris 2010 door using the FMVSS 214 standard [4]. This was achieved by pushing the door perpendicularly at a velocity of 8 m/s in 92 ms into a steel bar with a diameter of 254 mm. Setiawan et al. analyzed the door strength of an electric city car prototype using the Euro NCAP standard [5]. This involved pushing the door at a 75-degree angle on a horizontal plane at a velocity of 20 mph (8.94 m/s) in 80 ms into a steel bar with a diameter of 254 mm. Prem Kumar et al. analyzed the strength of a car door design specifically made to withstand a side impact of 8000 N, following the FMVSS

214 standard [6]. The results were obtained without considering the price of the materials used, and S-Glass Fiber was found to be the most applicable in terms of weight and strength compared to aluminum alloy and E-Glass Fiber. Ezkelia et al. analyzed the strength of a car door using the door slam method [7]. This involved slamming the door onto a stiff surface with an acceleration of 350 m/s² in 0.1 seconds. Patil et al. also employed the door slam method but with different parameters, utilizing an angle of 20 degrees, a velocity of 1 m/s, in 0.35 seconds [8].

In this research, a design for a car door will be created and tested using three simulation methods to assess its strength. These methods include pole side impact, side impact, and door slam tests. The simulations will be conducted using ANSYS 2019 R3 software, employing materials such as aluminum alloy 6061 T4, Type-E Fiberglass, and Type-S Fiberglass. The objective of this research is to identify a contest car door design that is safe, lightweight, and economically viable for use in an energy-saving vehicle competition.

2. Methodology

Figure 1 showed the car door design that was tested in this paper. The size of the door was set at 77 cm × 87 cm with a thickness of 2.9 mm as advised by the rules of the competition.

Figure 1. Car door design (unit in mm).

In this research, simulation was performed using three types of materials which were aluminum alloy, type-E fiberglass, and type-S fiberglass. Aluminum alloy 6000 series was the commonly used type as a body panel. The 6000 series aluminum alloys were known for their good formability, moderate strength, and corrosion resistance [9]. These alloys were heat treatable and alloyed with magnesium and silicon if required, which could lead to the precipitation of secondary phases such as Al_3Sc, Al_3Zr, and Mg_2Si, resulting in improved mechanical strength and comparable properties to the 5000 and 7000 series aluminum alloys [10]. Additionally, the 6000 series aluminum alloys had been extensively studied due to their better strength, weldability, corrosion resistance, and cost compared to other aluminum alloys [11]. However, it was important to note that these alloys could develop susceptibility to intergranular corrosion because of improper heat treatments or alloying [9].

The other types of materials, type-E fiberglass and type-S fiberglass were also tested. The mechanical and thermal properties of fiberglass-reinforced composites were influenced by the type of fiberglass used and the orientation of the fibers within the composite material [12,13]. Additionally, the amount of fiberglass incorporated into the composite material played a critical role in balancing mechanical strength and thermal conductivity [14]. Furthermore, the fabrication process and the adjustment of fiberglass contents could significantly impact the compressive strength and thermal insulation properties of porous ceramics [15]. Type-E fiberglass was known for its effective tensile properties and adhesive strength, making it suitable for reinforcing polymer composites [16,17]. On the other hand, type-S fiberglass was recognized for its superior mechanical properties, including high strength and modulus values, which made it ideal for applications requiring exceptional mechanical performance [17]. Each material's properties comparison was shown in Table 1.

This research was done using Solidworks 2020 SP4 software for the modeling of the car door design. The strength analysis was simulated using ANSYS 2024 R1 (Research License) software using the mechanical function of Finite Element Method (FEM) analysis. Three simulations were conducted to analyze the structural integrity of the car door. The prescribed simulation tests employed were delineated as follows. Firstly, the Pole Side Impact

Test was executed by exerting a perpendicular force on the door at a velocity of 8 m/s within a time frame of 92 ms. This force was applied onto a steel bar possessing a diameter of 254 mm. Secondly, the Side Impact Test was performed by subjecting the door to a uniform force of 8000 N. Lastly, the Door Slam Test was conducted by imparting an acceleration of 350 m/s² to the door within a time span of 0.1 seconds.

Table 1. Mechanical properties of the door material.

Materials	Density (kg/m³)	Young Modulus (GPa)	Poisson's Ratio	Tensile Strength (MPa)	Yiel Strength (MPa)
Aluminium alloy, wrought, 6061, T4 [18]	2713	68.9	0.33	241	145
Composite, PA12/E-glass fiber, woven fabric, biaxial [19]	1749	19.54	0.1049	4700	-
Composite, Epoxy/S-glass fiber, UD prepreg, QI [19]	1904	19.97	0.3065	1950	-

Other than the Finite Element Method simulation results, price estimation of the material used also became a deciding factor when comparing the end results. Price estimation calculation was performed using Equation 1. Where P_{T-Al} was the total price of aluminum alloy in IDR, P_{Al} was the aluminum alloy price per kg in IDR/kg, and w_{Al} was the weight of the aluminum alloy used in kg.

$$P_{T-Al} = P_{Al} \times w_{Al} \tag{1}$$

For type-E Fiberglass and type-S Fiberglass, both materials consisted of two base elements which were fiber and matrix (binder). The percentages of fiber determined the load-bearing capacity of the composite and load transformation capabilities depending on the contents of the matrix. A type-E fiber mat as reinforcement and the polyester resin with 65% fiber composite provided maximum impact strength of 12.6 Joule and 51.46 MPa stress concentration with 1.4 mm deformation [20]. Based on that, the ratio of the fiber and matrix elements in this study was decided to be 63.20% : 36.80%. The matrix element also consisted of two other elements which were resin and catalyst with the ratio of 90% : 10%. To estimate the cost of fiber, the weight of fiber was multiplied by the price of fiber per kg shown in Equation 2. Where P_{T-fg} was the total cost of fiber in IDR, P_{fg} was the price of fiberglass per kg in IDR/kg, $\%_{fg}$ was the percentage of fiberglass, and w_{fg} was the weight of fiberglass in kg.

$$P_{T-fg} = P_{fg} \times \left(\%_{fg} \times w_{fg} \right) \tag{2}$$

Equations 3 and 4 were used to calculate the total cost of the matrix. Where P_{Mat} was the total cost of the matrix in IDR, P_R was the resin price per kg in IDR/kg, P_C was the catalyst price per kg in IDR/kg, $\%_R$ was the percentage of resin, $\%_C$ was the percentage of catalyst, $\%_M$ was the total percentage of the matrix, and W_M was the total weight of the matrix used in kg.

$$P_{Mat} = [P_R \times (\%_R \times W_M)] + [P_C \times (\%_C \times W_M)] \tag{3}$$

$$W_M = \%_M \times w_{fg} \tag{4}$$

3. Result and Discussion

Firstly, the determination of the material cost is carried out by taking into consideration the mass of the car door. The mass of each individual material employed in the construction process is depicted in Table 2, utilizing the Solidworks 2020 SP4 software. In addition, Table 3 presents the current market availability and corresponding costs of the materials and resins at the time of the production of this study. Based on the computation employing equations (1) – (4), the aggregate cost necessary for each substance is exhibited in Fig. 2. Concerning the fiberglass calculation, the proportion of fiberglass and matrix element stands at 63.20% : 36.80%, whereas the proportion of catalyst and resin in the matrix element is 10% : 90%. After the computation, it is ascertained that the substances are ordered from the most expensive to the least expensive as follows: aluminum 6001-T4 (Rp 179,102.55), type-S Fiberglass (Rp 135,397.50), and type-E Fiberglass (Rp 127,182.99).

Table 2. Car door mass based on materials.

Material	Car door mass (kg)
Aluminum Alloy 6061-T4	3.743

Type – E Fiberglass	2.516
Type – S Fiberglass	2.716

Table 3. Cost of materials.

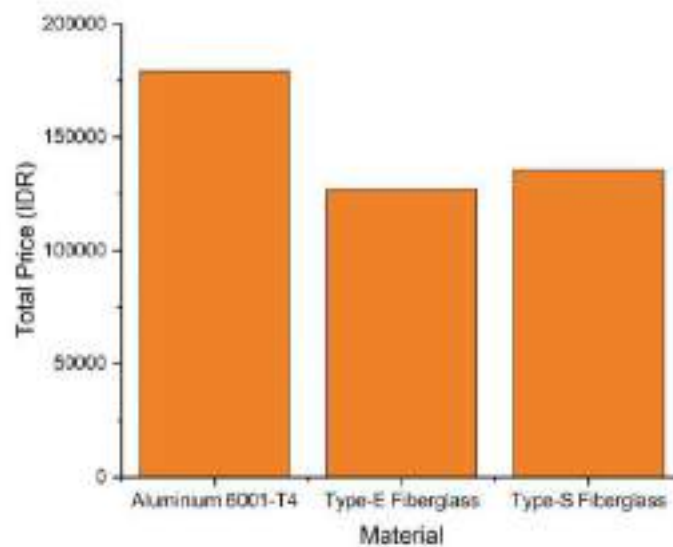| Material	Cost of Materials
Aluminum Alloy 6061-T4	US$ 3.3 / kg (IDR 47,850 / kg*)
Type – E Fiberglass [21]	US$ 1.5 / kg (IDR 21,750 / kg*)
Type – S Fiberglass [22]	US$ 1.0 / kg (IDR 14,500 / kg*)
Material	Cost of Materials
Resin [23]	IDR 55,100 / kg
Catalyst [24]	IDR 105,000 / kg

(*Exchange rate $1= Rp 14,500)

Figure 2. Total cost of materials.

Secondly, the evaluation of the outcomes obtained from the simulations of deformation and stress is thoroughly deliberated. This evaluation encompasses an in-depth analysis of the results derived from the pole side impact test, side impact test, and door slam test.
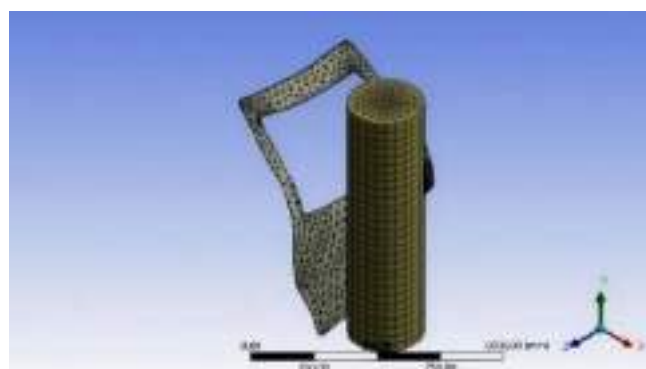

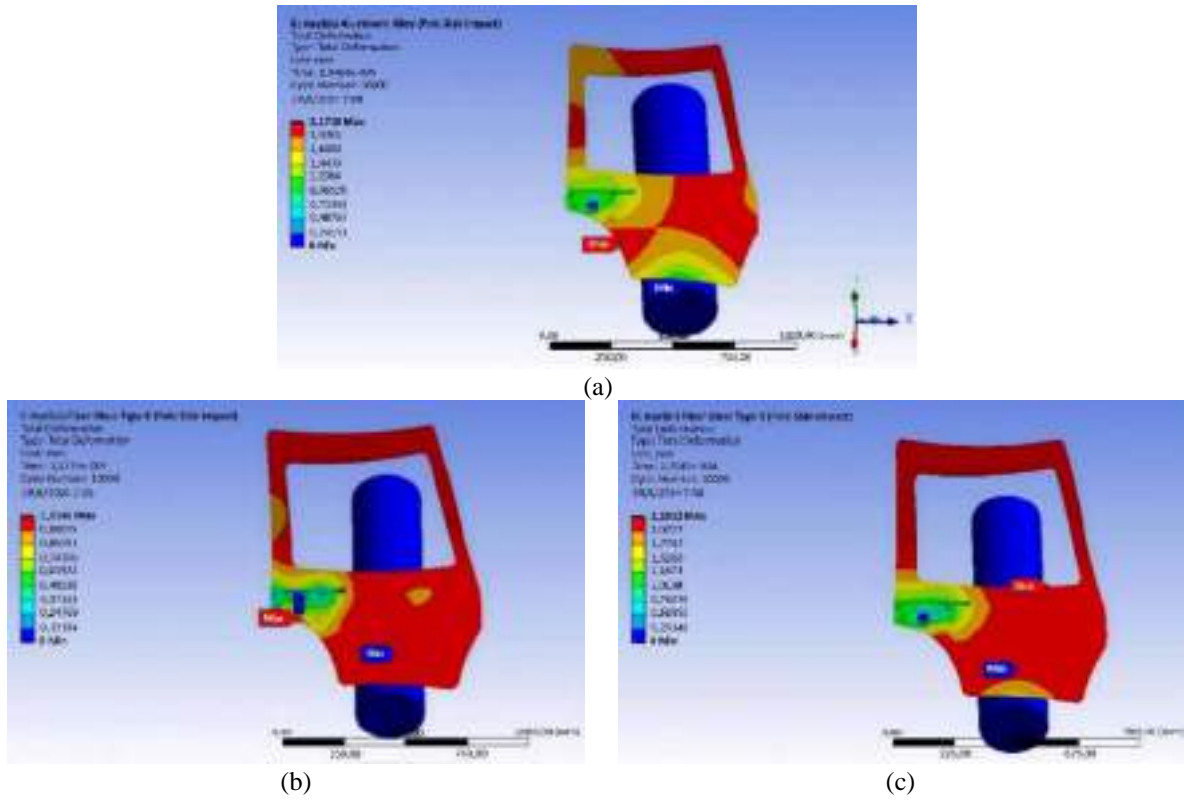Figure 3. Meshing results for pole side impact test simulation.

(a)

(b)

(c)

Figure 4. Total deformation results of side pole impact test simulation for (a) aluminum 6001-T4, (b) type E-fiberglass, and (c) type-S fiberglass.
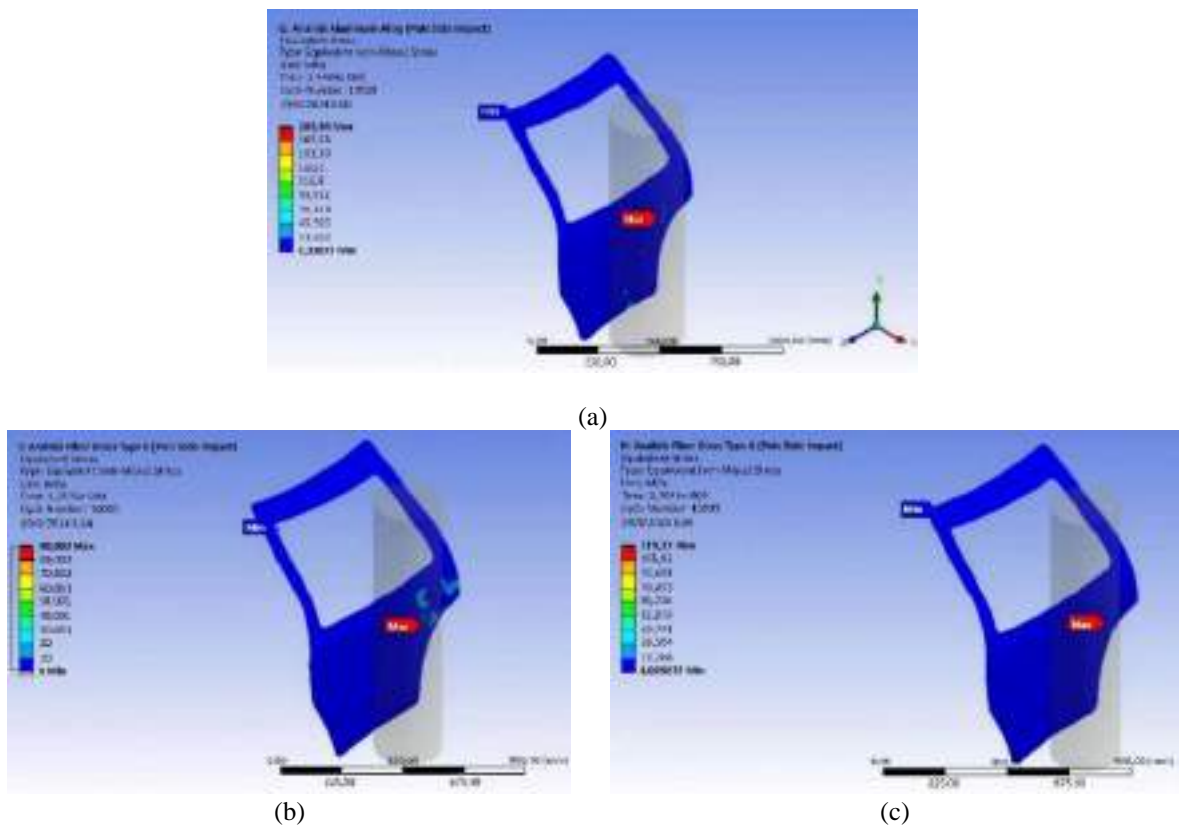

(a)

(b)

(c)

Figure 5. Von Mises stress results of side pole impact test simulation for (a) aluminum 6001-T4, (b) type-E fiberglass, and (c) type-S fiberglass.

Figure 3 depicts the meshing of the pole side impact simulation. The mesh used for the door comprises 18,269 elements with 43,453 nodes. The results of the simulation unveil the total deformation and von Mises stress values, as presented in Figs. 4 and 5, respectively. Notably, the aluminum 6001-T4 records a maximum total deformation of 2.1718 mm, while type-E fiberglass and type-S fiberglass register total deformations of 1.1146 mm and 2.2812 mm, respectively. Evidently, the fiberglass materials exhibit a broader extent of deformation compared to the aluminum 6001-T4 because fiberglass has a lower modulus of elasticity while having higher tensile strength. Thus, aluminum is stiffer than fiberglass. The type-S fiberglass material achieves the highest total deformation, whereas the type-E fiberglass material records the lowest.

When assessing the von Mises stress, the maximum values for each material are 209.98 MPa, 90.002 MPa, and 119.17 MPa for aluminum 6001-T4, type-E fiberglass, and type-S fiberglass, respectively, as illustrated in Fig. 5. As indicated by the simulation results, each door exhibits a single point of maximum value. Consequently, the door materials display a relatively low average von Mises stress. Comparatively, aluminum 6001-T4 exhibits the highest von Mises stress among the materials, while type-E fiberglass exhibits the lowest stress.

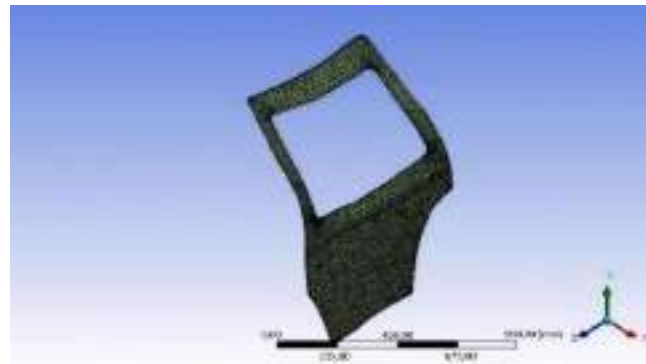Figure 6. Meshing results for side impact test simulation.

(a)

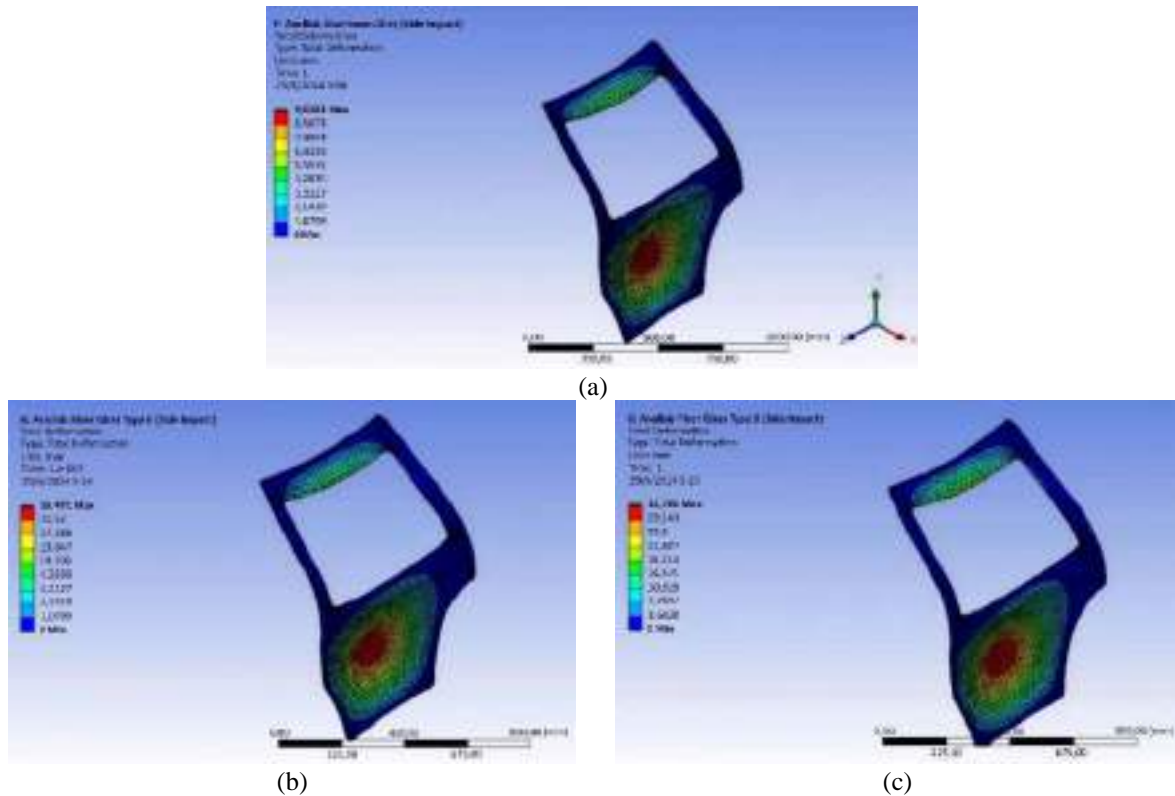(b)   (c)

Figure 7. Total deformation results of side impact test simulation for (a) aluminum 6001-T4, (b) type E-fiberglass, and (c) type-S fiberglass.

The illustration in Fig. 6 depicts the meshing utilized for the simulation of the side impact test. In Fig. 7, the utmost degree of deformation is observed for each material, with values of 15.658 mm, 56.753 mm, and 52.457 mm, corresponding to aluminum 6001-T4, type-E fiberglass, and type-S fiberglass, respectively. It should be noted that all materials exhibit their highest deformation in the lower middle portion of the door. Interestingly, the type-E fiberglass attains the highest deformation value, whereas the aluminum 6001-T4 achieves a comparatively lower deformation value.

For the von Mises stress, the values of 266.41 MPa, 590.06 MPa, and 595.49 MPa are observed for aluminum 6001-T4, type-E fiberglass, and type-S fiberglass respectively, as depicted in Fig. 8. It is noteworthy that fiberglass exhibits twice the von Mises value compared to aluminum 6001-T4. The stress area distribution reveals that most of the area is colored light green and blue, implying that all materials experienced a moderate level of stress. The maximum von Mises stress was only observed in a small portion of the door. Notably, type-S fiberglass exhibited the highest von Mises stress value among the various materials, whereas the aluminum 6001-T4 achieved the lowest value.
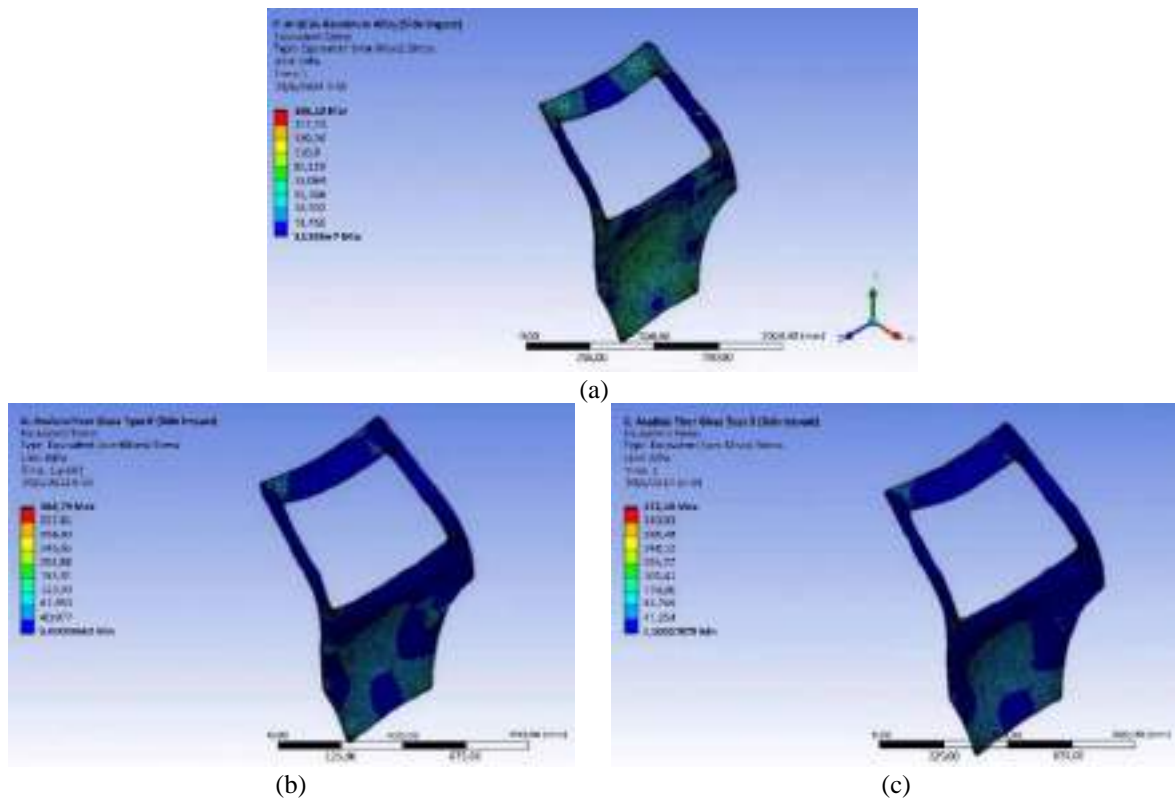

(a)

(b)

(c)

Figure 8. Von Mises stress results of side impact test simulation for (a) aluminum 6001-T4, (b) type-E fiberglass, and (c) type-S fiberglass.

Figure 9. Meshing results for door slam test simulation.

(a)

(b)   (c)
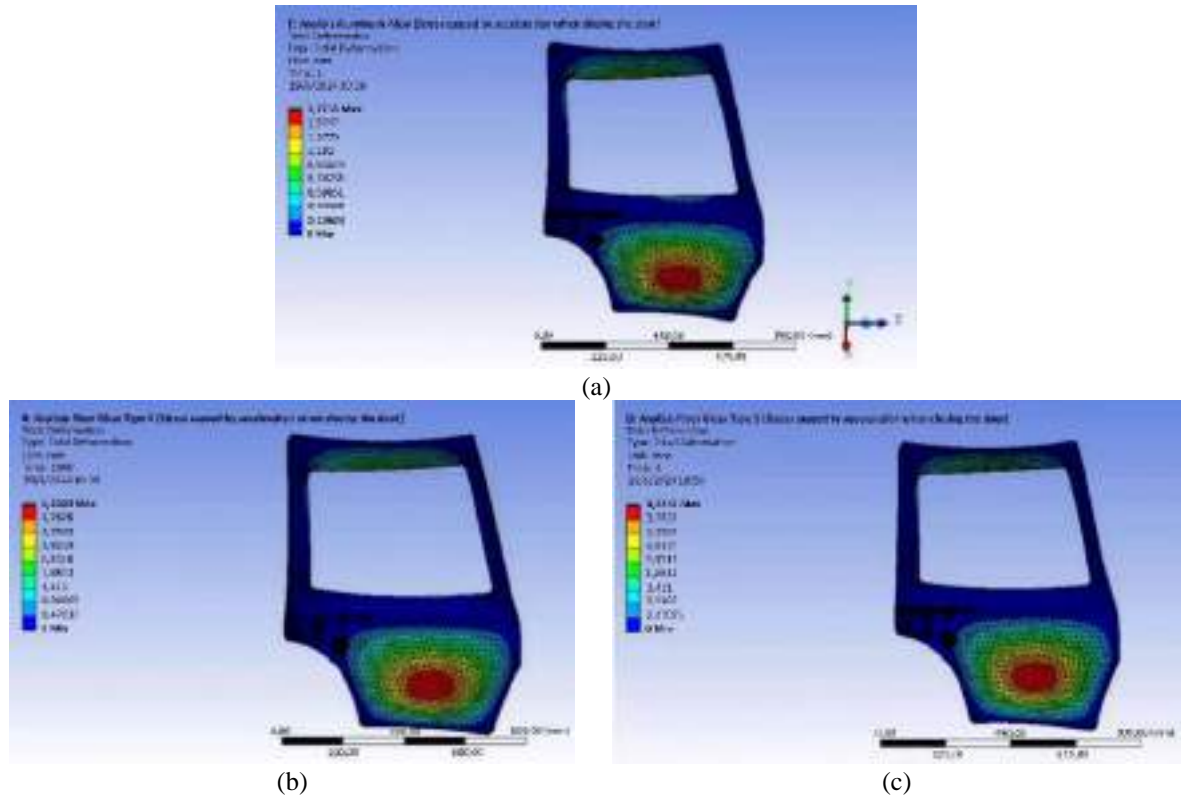
Figure 10. Total deformation results for door slam test simulation for (a) aluminum 6001-T4, (b) type E-fiberglass, and (c) type-S fiberglassv.

(a)

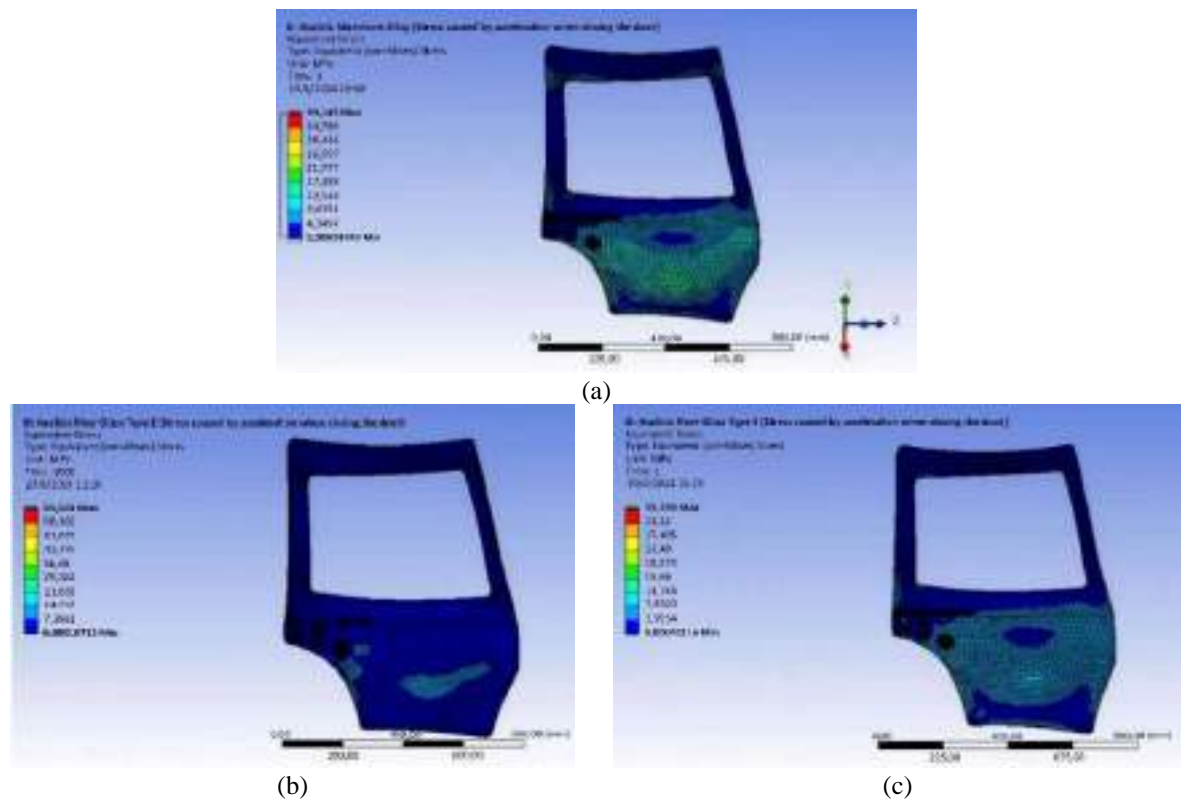(b)   (c)

Figure 11. Von Mises stress results for door slam test simulation for (a) aluminum 6001-T4, (b) type-E fiberglass, and (c) type-S fiberglass.

Figure 9 depicts the meshing utilized in the simulation for the door slam test. The maximum value of total deformation observed for aluminum 6001-T4 is 1.7715 mm, while for type-E fiberglass it is 4.2329 mm, and for type-S fiberglass it is 4.2331 mm. It can be observed that the fiberglass materials exhibit a broader region of deformation when compared to aluminum 6001-T4. In Fig. 10, it is illustrated that the most significant deformation occurs in the bottom middle section of the door, which corresponds to the findings of the side impact test. In this observation, the fiberglass materials attain the highest maximum value for total deformation.

The von Mises stress, as portrayed in Fig. 11, reaches its peak values of 39.145 MPa, 65.664 MPa, and 35.235 MPa for aluminum 6001-T4, type-E fiberglass, and type-S fiberglass, respectively. This stress is induced by the acceleration experienced during the door closing process. Notably, among all the materials, type-E fiberglass exhibits the highest von Mises stress, while type-S fiberglass registers the lowest value. In this study, von Mises stress is preferred over engineering stress because the car door experiences multiaxial stress states or plastic deformation. It provides a more accurate representation of the stress state and can help in predicting material failure under complex loading conditions, which are common in many engineering applications.

Figures 12 and 13 display the maximum values of deformation and strength comparison obtained from all test materials and all three methods. The side impact test yields the highest deformation and stress, whereas the pole side impact results in the lowest deformation. However, the door slam test exhibits the lowest von Mises stress compared to the other methods. Despite these variations, all three materials can withstand the stress from the side impact test as the stress value remains below the tensile strength of each material.
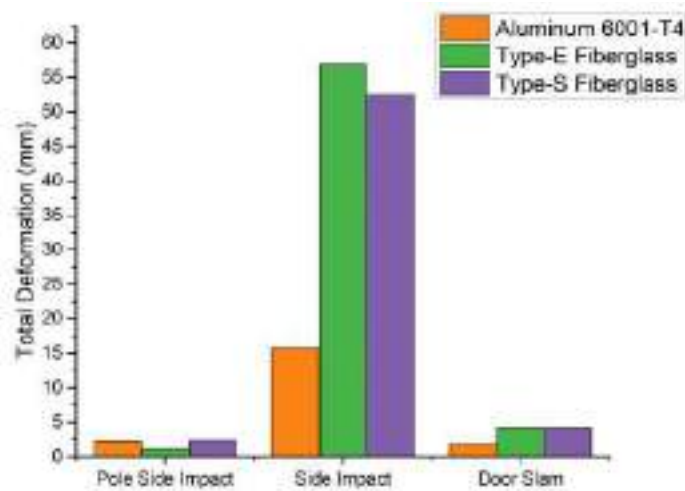

Figure 12. Comparison of maximum deformation values for three types of door materials in three testing methods.
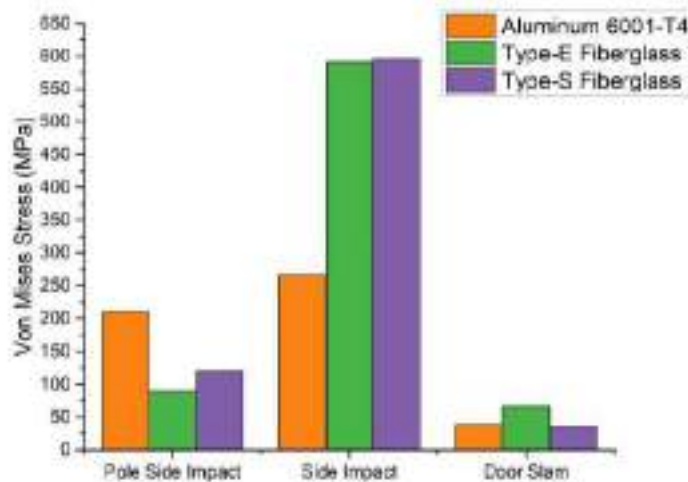

Figure 13. Comparison of maximum von Mises stress values for three types of materials in three testing methods

During the Pole Side Impact test, aluminum's higher stiffness, represented by its greater Young's modulus, along with its ability to deform locally, leads to higher von Mises stress. On the other hand, fiberglass composites, which have a lower modulus of elasticity and better energy distribution properties due to their Poisson's ratio and material structure, experience lower stress. In the Side Impact test, aluminum's higher modulus of elasticity enables it to distribute uniform loads more effectively, resulting in lower von Mises stress compared to fiberglass composites. The latter, with their lower modulus and less uniform load distribution capabilities, exhibit higher stress under the same loading conditions.

To establish a ranking for each material, it is imperative to establish specific criteria. These criteria comprise the strength of the door in the pole side impact, which accounts for 25% of the evaluation, the strength of the door in the side impact, also accounting for 25% of the evaluation, the cost of the material, which contributes 25% to the evaluation, and the mass of the material, which also contributes 25% to the evaluation. It is worth noting that the strength results obtained from the door slam test will not be considered in the evaluation criteria. This decision is based on the simulation results, which indicate that the door strength is minimally affected by the test and therefore holds little value. The results of the evaluation of the three different materials are presented in Table 4. The data show that type-E fiberglass yields the highest value of 2.75.

Table 4. Total material weight values according to simulation results.

Material/Parameter	Pole Side (25%)	Side Impact (25%)	Mass (25%)	Cost (25%)	Rank Value	Safety Factor
Aluminum	1	1	1	1	1	0.54
Type-E Fiberglass	3	2	3	3	2.75	7.97
Type-S Fiberglass	2	3	2	2	2.25	3.28

Safety factor calculation in Table 4 is defined as the yield strength (for aluminum alloy) or tensile strength (for fiberglass) of the material divided by the maximum von Mises stress in the side impact test since it produces the largest stress in the test. Type-E Fiberglass and Type-S Fiberglass achieved a safety factor above 1, which is within the general range of mechanical design safety factors of 1.5 – 2 [25]. Type-E fiberglass has the highest safety factor. Consequently, it can be concluded that type-E fiberglass is the most suitable material for utilization as the car door in the energy-saving car prototype.

4. Conclusion

The car door design has undergone comprehensive strength testing utilizing three different methods—pole side impact, side impact, and door slam tests—employing three distinct materials: aluminum 6001-T4, type-E fiberglass, and type-S fiberglass. The results of these tests have provided critical insights into the performance and suitability of each material for use in energy-efficient vehicle prototypes.

The pole side impact test revealed that aluminum 6001-T4 experienced the highest levels of stress and deformation among the tested materials. This outcome is attributed to aluminum's higher stiffness and localized deformation characteristics, which result in elevated von Mises stress values under concentrated impact conditions.

In the side impact test, both type-E and type-S fiberglass materials exhibited significantly higher stress and deformation compared to aluminum 6001-T4. The lower modulus of elasticity in fiberglass materials, coupled with their less effective load distribution capability, accounts for the increased von Mises stress observed in these tests.

The door slam test indicated minimal deformation and stress across all three materials. However, type-E fiberglass recorded the highest levels of stress and deformation, although these values remained relatively low overall. This test further highlighted the robustness of aluminum 6001-T4 in withstanding dynamic loads during door closure scenarios.

A comprehensive evaluation considering the generated stress, overall mass, and material cost was conducted to determine the most suitable material for the car door prototype. Type-E fiberglass emerged as the optimal choice due to its superior balance of cost-effectiveness, lightweight properties, and adequate strength. Its higher safety factor and satisfactory performance in all conducted tests affirm its suitability for use in energy-efficient vehicle designs.

In conclusion, while aluminum 6001-T4 demonstrated excellent stiffness and strength under certain impact conditions, type-E fiberglass offers a more balanced combination of properties, making it the most appropriate material for the car door in the context of energy-saving vehicles.

References

[1]   A. Robinson, A. Taub, and G. Keoleian, "Fuel efficiency drives the auto industry to reduce vehicle weight", MRS Bulletin, vol. 44, no. 12, pp. 920-923, 2019, doi: 10.1557/mrs.2019.298.

[2]   Universitas Negeri Malang, "Peraturan KMHE 2019". Malang: Kementerian Riset, Teknologi, dan Pendidikan Tinggi Republik Indonesia, 2019.

[3]   I. Shikkerimath, "Studies on Structural Analysis of Automotive Door Using Conventional, Present and Proposed Materials," Int J Res Appl Sci Eng Technol, vol. 6, no. 1, pp. 1901–1906, Jan. 2018, doi: 10.22214/ijraset.2018.1295.

[4]   C. R. Long, S. C. K. Yuen, and G. N. Nurick, "Analysis of a car door subjected to side pole impact," Latin American Journal of Solids and Structures, vol. 16, no. 8, pp. 1–17, 2019, doi: 10.1590/1679-78255753.

[5]   R. Setiawan and M. R. Salim, "Crashworthiness Design for an Electric City Car against Side Pole Impact," Journal of Engineering and Technological Sciences, vol. 49, no. 5, pp. 587–603, Nov. 2017, doi: 10.5614/j.eng.technol.sci.2017.49.5.3.

[6]   P. D, V. Balaji, M. M. Sherief, C. M, and B. Hariharan S, "Design and impact analysis of car door," International Journal of Creative Research Thoughts, vol. 6, no. 1, pp. 270–276, 2018.

[7]   E. E, A. A, and D. Tilahun, "Finite Element Analysis of Internal Door Panel of a Car by Cons idering Bamboo Fiber Reinforced Epoxy Composite," J Appl Mech Eng, vol. 06, no. 01, pp. 1–6, 2017, doi: 10.4172/2168-9873.1000247.

[8]   S. S. Patil and G. U. Dhuri, "Assessment of Automobile Door Slam using Finite Element Method," International Journal of Innovative Technology and Exploring Engineering, vol. 9, no. 4, pp. 348–355, Feb. 2020, doi: 10.35940/ijitee.D1195.029420.

[9]   M. Cornejo, T. Hentschel, D. Koschel, C. Matthies, L. Peguet, M. Rosefort, C. Schnatterer, E. Szala, and D. Zander, "Intergranular corrosion testing of 6000 aluminum alloys", Materials and Corrosion, vol. 69, no. 5, pp. 626-633, 2017, doi: 10.1002/maco.201709813.

[10]   S. L. Sing, and W. Y. Yeong, "Laser powder bed fusion for metal additive manufacturing: perspectives on recent developments", Virtual and Physical Prototyping, vol. 15, no. 3, pp. 359-370, 2020, doi: 10.1080/17452759.2020.1779999.

[11]   H. Lin, J. R. Hwang, C. P. Fung, "Fatigue Properties of 6061-T6 Aluminum Alloy T-Joints Processed by Vacuum Brazing and TIG Welding", Materials Transactions, vol. 57, no. 2, pp. 127-134, 2016, doi: 10.2320/matertrans.M2015343.

[12].   A. Nassar, and E. Nassar, "Effect of fiber orientation on the mechanical properties of multi layers laminate nanocomposites", Heliyon, vol. 6, no. 1, e03167, 2020, doi: 10.1016/j.heliyon.2020.e03167.

[13]   T. Yasue, N. Iwasaki, M. Shiozawa, Y. Tsuchida, T. Suzuki, and H. Takahashi, "Effect of fiberglass orientation on flexural properties of fiberglass-reinforced composite resin block for cad/cam", Dental Materials Journal, vol. 38, no. 5, pp. 738-742, 2019, doi: 10.4012/dmj.2018-249.

[14]   H. Avcı, and A. U. Ozdemir, "Sustainable approach to produce polyurethane composite foams with natural materials", Celal Bayar Üniversitesi Fen Bilimleri Dergisi, 2017, doi: 10.18466/cbayarfbe.293113.

[15]   S. Li, B. Chang, M. Li, and S. Ran, "Fabrication of high strength and thermal insulation porous ceramics via adjusting the fiberglass contents", International Journal of Applied Ceramic Technology, vol. 20, no. 4, pp. 2321-2330, 2023, doi: 10.1111/ijac.14343.

[16]   H. S. Ku, H. Wang, N. Pattarachaiyakoop, and M. Trada, "A review on the tensile properties of natural fiber reinforced polymer composites", Composites Part B: Engineering, vol. 42, no. 4, pp. 856-873, 2011, doi: 10.1016/j.compositesb.2011.01.010.

[17]   H. Churei, R. U. Chowdhury, Y. Yoshida, G. Tanabe, S. Fukasawa, T. Shirako, W. T. Wada, M. Uo, H. Takahashi, and T. Ueno, "Use of the fiberglass reinforcement method in thermoplastic mouthguard materials to improve flexural properties for enhancement of functionality", Dental Materials Journal, vol. 40, no. 6, pp. 1338-1344, 2021, doi: 10.4012/dmj.2020-402.

[18].   Matweb, "Aluminum 6061-T4; 6061-T451," *Matweb*. https://www.matweb.com/search/DataSheet.aspx?MatGUID=d5ea75577b1b49e8ad03caf007db5ba8 (accessed Oct. 12, 2023).

[19]   ANSYS, "Material Properties - Granta Design." ANSYS, 2019.

[20]   S. Asmare, B. Yoseph, and T. M. Jamir, "Investigating the impact resistance of E-glass/ Polyester composite materials in variable fiber-to-matrix weight ratio composition", Cogent Engineering, vol. 10, no.1, 2023, doi: 10.1080/23311916.2023.2178110.

[21]   L. Hebei Yuniu Fiberglass Manufacturing Co., "Fiberglass material E glass Fiberglass Chopped Strand Mat EMC300-600," *Alibaba*. https://www.alibaba.com/product-detail/Fiberglass-Material-Fiberglass-Material-E-Glass_1700007720100.html?spm=a2700.7735675.normal_offer.d_image.5a3866e3a6Xwjy&s=p (accessed Jun. 08, 2022).

[22]   L. Jiujiang Beihai Fiberglass Co., "Serat Kaca S Kekuatan Tinggi," *Alibaba*. https://indonesian.alibaba.com/p-detail/High-735543205.html?spm=a2700.galleryofferlist.normal_offer.d_image.10b36d820yIcFk (accessed Jun. 08, 2022).

[23]   jakartakimia, "Resin Bening 1Kg + Katalis 20 Gram - Resin Bening - Resin Polyester - Kerajinan Tangan," *Lazada*. https://www.lazada.co.id/products/resin-bening-1kg-katalis-20-gram-resin-bening-resin-polyester-kerajinan-tangan-i5370838454-s10588292641.html?freeshipping=1&search=1&spm=a2o4j.searchlist.list.2 (accessed Jun. 10, 2023).

[24]   KimiaID, "Katalis Resin - Katalis MEPOXE," *Bukalapak*. https://www.bukalapak.com/p/industrial/industrial-lainnya/1macrki-jual-catalyst-1-liter-katalis-resin-katalis-mepoxe-katalis-polyester-resin-pengering-resin-fiber-katalis-resin-fiber-katalis-resin-bening?from=list-product&pos=4 (accessed Jun. 10, 2023).

[25]   R. Budynas, and K. Nisbett, "*Shigley's mechanical engineering design*", Eight Edition, McGraw-Hill, 2008.

JESCEE
Journal of Emerging Supply Chain, Clean Energy, and Process Engineering

RELIABILITY EVALUATION OF ELECTRIC POWER GENERATION PLTS SYSTEM ON PUBLIC STREET LIGHTING TARAKAN CITY

M. Tesar Apriliandy[1*], Achmad Budiman[2]
[1]Department of Electrical Engineering, Faculty of Engineering, University of Borneo Tarakan, North Kalimantan, Indonesia
[2]Department of Electrical Engineering, Faculty of Engineering, University of Borneo Tarakan, North Kalimantan, Indonesia

Abstract
Public street lighting (PJU) is a lighting lamp that is public (for the common good) and is usually installed on the road. Solar Public Street Lighting (PJU-TS) is a public street lighting where the electrical power for the lights is supplied by a Stand Alone system that uses solar energy. In this study, measurements of sunlight, lamplight intensity, and lamppost height were carried out on 24 PJU-TS units spread across 4 sub-districts in Tarakan city. Furthermore, simulating PJU-TS using Matlab Simulink to determine the level of reliability based on the use or usage of batteries in PJU-TS. Based on the regulation of the Minister of Transportation of the Republic of Indonesia Number PM 27/2018 concerning Street Lighting Equipment that the lighting level of PJU-TS lamps is 3-6 lux and based on recommendations from the Reliability Standard Power Plant that the reliability value is at least 80%. The results of this research simulation that PJU-TS that meets the standards of the Minister of Transportation of the Republic of Indonesia Number PM 27/2018 amounted to 3 units of 3-6 lux, 40 W lamps, lamp working hours 11 hours 14 minutes, 300 WP solar modules, solar charge controller current 15.72 A, 40 Ah batteries, battery working hours 13.72-18.68 hours, percentage of Ah battery usage 46.42% - 95%. In addition to meeting the standards of the Minister of Transportation of the Republic of Indonesia Number PM 27/2018, the results of this simulation also meet the Reliability Standard Power Plant recommendations with reliability exceeding 80%, namely 81.27% - 100%. Meanwhile, 21 units of PJU-TS do not meet the standards of the Minister of Transportation of the Republic of Indonesia Number PM 27/2018 concerning Street Lighting Equipment and Reliability Standard Power Plant recommendations.

1. Introduction

This modern era cannot be separated from the existence of energy. All of it is a support for our daily lives that allows our lives to be easier, more practical and efficient. One of the renewable energies is solar energy where many consumer communities have used it. Indonesia, as a tropical country with an average of 12 hours of sunshine per day, has tremendous potential for solar energy. According to the National Energy General Plan (RUEN), Indonesia has an estimated solar energy potential of 207,898 MW (4.80 kWh/m2/day), equivalent to 112,000 GWp. One of the uses of electricity that is widely used by people today is as a source of lighting. The increasing level of community mobility makes all activities require lighting, including highways or public roads. Public street lighting is lighting that is public (for the common good) and is usually installed on roads or in certain places such as parks, and other public places. Public Street Lighting (PJU). PJU (Public Street Lighting) Solar Power is a public street lighting where the electrical power for the lights is supplied by an independent system obtained from solar energy. The reliability of electrical power generation in the PLTS system plays an important role in meeting

the needs for Public Street Lighting (PJU). A good level of reliability determines the continuity of the PLTS system's electrical power distribution on Public Street Lighting (PJU).

2. Experimental Section

A. Place and Time of Research

This research will be carried out at points where the PLTS system is installed on public street lighting in the city of Tarakan. This research was carried out for approximately 6 months.

B. PJU-TS reliability

In this study, calculation analysis is carried out with the data that has been obtained, then simulate PJU-TS using matlab simulink to determine the level of reliability based on the use or use of batteries in PJU-TS. Based on the regulation of the Minister of Transportation of the Republic of Indonesia Number PM 27/2018 concerning Street Lighting Equipment that the lighting level of PJU-TS lamps is 3-6 lux and based on recommendations from the Reliability Standard Power Plant that the reliability value is at least 80%. If the equipment works at least 80%, it can be said to be reliable because the equipment works in minimum conditions so that a good capacity is if the equipment works at least 80%, with a maximum reliability value of 100% if the power plant equipment works in conditions of 80% of the power plant capacity. The theory in this research follows the title of the discussion to be researched, and references are obtained from journals, books, and others.

C. Solar Public Street Lighting (PJU-TS)

Solar public street lighting uses solar cell panels that function to receive sunlight and then convert it into electrical energy through the photovoltaic process. Photovoltaic systems produce output power only when the photovoltaic modules are illuminated by the sun, therefore photovoltaic systems use energy storage mechanisms so that electrical energy is always available when the sun is no longer shining (at night). The battery is a component used for storing the electrical energy produced by the photovoltaic array. In addition to being a storage medium for electrical energy, batteries are also used for system voltage regulation and current sources that can exceed the capabilities of photovoltaic arrays. The formula used is as follows:

Calculating Ornament Handlebar Angle   [1]

$$T = \sqrt{h^2 + c^2}$$

$$\cos^{-1} \varphi = \frac{h}{T}$$

With:

T = Distance of lights to the center of the road

h = Pole height

c = horizontal distance of the lamp to the center of the road

φ = Angle of inclination of the handlebar ornament

Calculating light intensity (i in candela/cd)

$$I = \frac{\phi}{\omega}$$

Then :

$$k = \frac{\Phi}{p} \text{ dan } \Phi = k \; x \; p$$

With:

I = Light intensity in candela (cd)

ϕ = Light flux in lumens (lm)

$\boldsymbol{\omega}$ = Angle of space in sterdian (sr)

Calculating Illumination Intensity

$$Ep = \frac{k \; x \; W \; x \cos\beta}{\omega \; x \; r^2}$$

With:

Ep = Illumination Intensity

K = Efficacy of light

W = Lamp power

Cos β = Angle of inclination of the handlebar ornament

$\boldsymbol{\omega}$ = Angle of space in sterdian (sr)

r = distance from light source to point P (m)

Calculating Solar Module Capacity: [2]

Module capacity (W) = Im x Vm

With:

Im = Panel maximum current

Vm = Maximum voltage of the panel

The size or rating for the flow control device in and out of the battery in Amperes is :

$$Icc = \frac{Pmaks}{FF \; x \; Voc} \; x \; (100\% + \text{η baterai})$$

With:

icc = solar charge controller rating current (amperes)

Pmax = many solar panels x Pnom (watts)

Calculate the battery capacity as follows:

$$\frac{Eload}{\eta v}$$

With:

Eload = Quantity of energy

η = Battery Efficiency

v = Battery voltage

D. Research Procedure

Data is obtained by direct observation and conducting interviews with the parties concerned. After obtaining the data, then the calculation analysis is carried out using the data that has been obtained after that the simulation is carried out using Matlab Simulink based on Reliability Standard Power Plant. f the equipment works at least 80%, it can be said to be reliable because the equipment works in minimum conditions so that a good capacity is if the equipment works at least 80%, with a maximum reliability value of 100% if the power plant equipment works in conditions of 80% of the power plant capacity.

3. Result and Discussion

There are 24 PJU-TS locations in 4 sub-districts of Tarakan city that have been installed by the Ministry of Energy and Mineral Resources and managed by the Tarakan city Transportation Office. In the east Tarakan sub-district there are 6 streetlights, in the middle Tarakan sub-district there are 4 streetlights, in the west Tarakan sub-district there are 6 streetlights, in the north Tarakan sub-district there are 8 streetlights. Based on the Road Classification according to the regulation of the Minister of Transportation of the Republic of Indonesia Number PM 27/2018 concerning Street Lighting Equipment at the PJU-TS location point in Tarakan city including Environmental roads. Based on the Road Classification according to the regulation of the Minister of Transportation of the Republic of Indonesia Number PM 27/2018 concerning Street Lighting Equipment at the PJU-TS location point of Tarakan city including Environmental roads. Environmental roads are public roads that serve environmental transportation with short distance travel characteristics, and low average speeds. The requirement for strong lighting (illumination) that must be produced for Environmental roads is 3-6 lux.

A. Solar Public Street Lighting Data

Calculating Ornament Handlebar Angle

With:

Pole height (h) = 7 m

Horizontal distance from the lamp to the center of the road (C) = 5 m

$$T = \sqrt{h^2 + c^2}$$

$$= \sqrt{7^2 + 5^2}$$

$$= 8,602 \ meter$$

Then :

$$\cos \varphi = \frac{h}{t}$$

$$= \frac{7}{8,602}$$

$$= 0,813$$

$$\varphi = \cos^{-1} 0,813$$

$$\varphi = 35,609°$$

Calculating light intensity (i in candela/cd)

$$I = \frac{\Phi}{\omega} \text{ or } \boldsymbol{\omega} = 4\pi$$

With :

$$k = \frac{\Phi}{p} \text{ dan } \Phi = k \; x \; p$$

$$i = \frac{k \; x \; p}{\omega}$$

$$= \frac{100 \; x \; 40}{4\pi}$$

$$= \frac{4000}{4\pi}$$

$$= 318,30 \text{ cd}$$

Calculating Illumination Intensity

With :

h   = 7 m

W   = 40 W

r^2 $= \sqrt{7^2 + 5^2} = 8,602$

          $= 8,602^2 = 74$

          $r^2 = 74$

$\cos \beta$ = 0,813

$\boldsymbol{\omega}$ $= 4\boldsymbol{\pi}$

$4\boldsymbol{\pi}$ = 4 x 3,14

$\boldsymbol{\omega}$ = 12,56

$$Ep = \frac{k \; x \; W \; x \cos\beta}{\omega \; x \; r^2}$$

$$= \frac{100 \; x \; 40 \; x \; 0,813}{12,56 \; x \; 74}$$

$$= \frac{3.252}{929,44}$$

$$= 3,49 \; lux$$

Solar Panels

The specifications of solar panels used in solar public street lighting in Tarakan city can be seen in Table 1. As follows:

Table 1. Solar Panel Specifications

Description	Specification
Type	*polycrystalline*
Module Power (Pnom)	300W
Max voltage (Vm)	36,41 V
Max current (Im)	8,24 A
No-load voltage (Voc)	45,20 V
Short circuit current (Isc)	8,73 A
Module dimensions	1956 mm x 982 mm

To find the value of the module capacity by multiplying the maximum current of the panel with the maximum voltage of the panel.

Module capacity (W) = Im x Vm

$= 8,24 \ x \ 36,41$

$= 300 \ W$

Solar Charge Controller

Table 2. Specifications of Solar Charge Controller

Description	Specification
Type	*Switching Regulator MPPT*
PV Module Input Voltage	Max. 45 VDC
Max Charge Current	15 A
Battery Input Voltage	Max. 29,4 VDC
Upper Limit Voltage	12,6 V - 13,8 V (12 V System) 27.6 V – 29,4 V (24 V System)

The size or rating for the flow control device in and out of the battery in Amperes is :

$$\text{Icc} = \frac{Pmaks}{FF\ x\ Voc} \ x \ (100\% + \ \text{n baterai})$$

$$= \frac{300}{0,76\ x\ 45,20} \ x \ (100\% + 80\%)$$

$$= \frac{300}{34,35} \ x \ 1,8$$

$$= 15,72\ A$$

Battery

<div align="center">Table 3 Battery Specifications</div>

Description	Specification
Type	*Battery LifePO4* (*Lithium -ion ferrouse phosphate*)
Voltage	25,6 V
Current Capacity	40 AH
Battery Efficiency	80 %

Calculating the capacity of the battery used:

$$\frac{Eload}{\text{n v}} = \frac{768\ wh}{80\%\ x\ 24\ V}$$

$$= 40\ Ah$$

B. Modeling PJU-TS Using Matlab Simulink Based on Field Data

Simulink modeling with lighting intensity using measurement results measured using measuring instruments
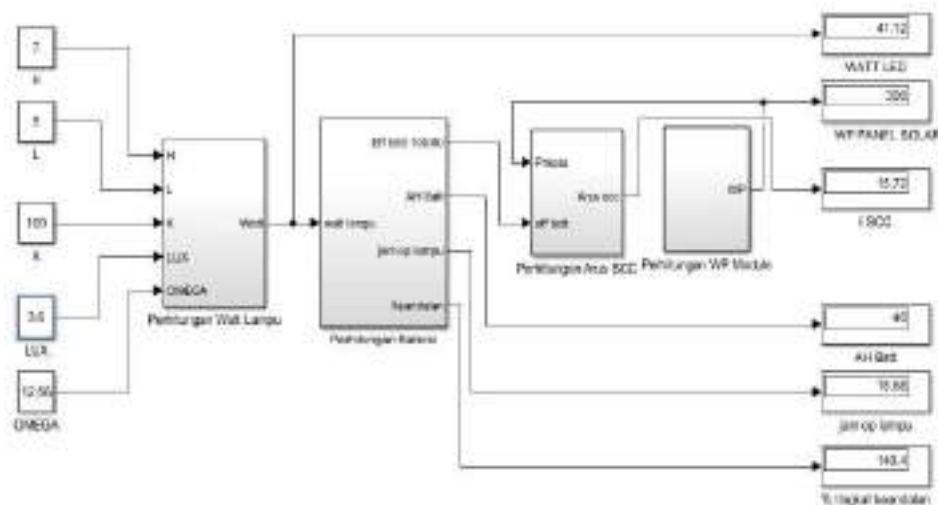

Figure 1. Subsystem modeling results based on measurement results

Figure 2. Graph of Modeling Results for the Central Tarakan subsystem
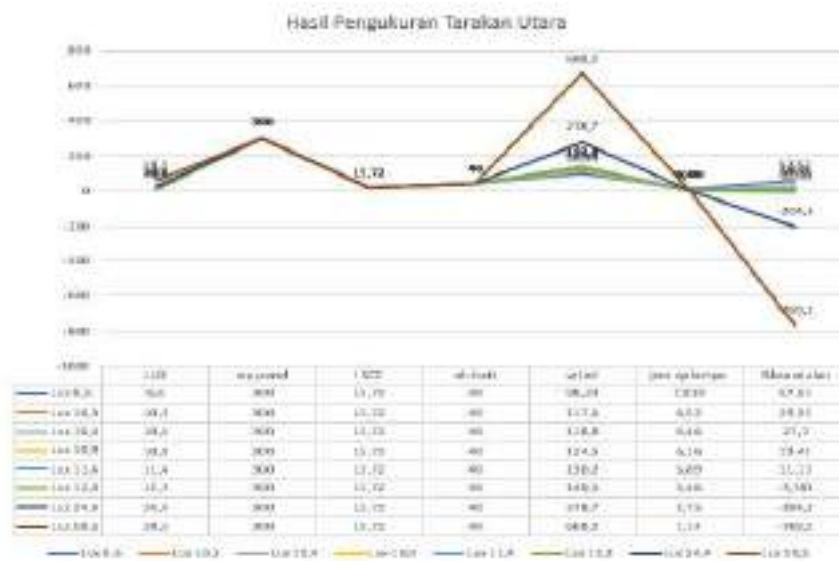

Figure 3. Graph of Modeling Results for the North Tarakan subsystem

Figure 4. Graph of Modeling Results for the West Tarakan subsystem

Figure 5. Graph of Modeling Results for the East Tarakan subsystem

Table 4. Battery Usage and Reliability

NO.	Battery Usage (%)	Working hours Lamp	Reliability (%)
1.	46,42 %	11 hours 14 minutes	100 %
2.	50 %	12 hours	100 %
3.	60 %	14 hours 4 minutes	100 %
4.	65 %	15 hours 6 minutes	100 %
5.	70 %	16 hours 8 minutes	100 %
6.	75 %	18 hours	100 %
7.	80 %	19 hours 2 minutes	100 %
8.	85 %	20 hours 4 minutes	93,7 %
9.	90 %	21 hours 6 minutes	87,51 %
10.	95 %	22 hours 8 minutes	81,27 %
11.	100 %	24 hours	75 %

From the table above it can be seen that the amount of usage or use of the battery can affect the working hours of the battery and the level of reliability of the battery. The use of a good battery if the battery works at least 80% of its capacity so that it affects the capacity and lifetimenya or battery life.

Based on mathematical modeling using Matlab Simulink that the field data of lamp working hours is 11 hours 14 minutes, it is known that the battery usage is only 46.42% with the remaining battery usage of 53.58% and a reliability level of 100%.

4. Conclusion

Based on the results of research conducted by simulating PJU-TS using Matlab Simulink that PJU-TS that meets the standards of the Minister of Transportation of the Republic of Indonesia Number PM 27/2018 totals 3 units of Solar Public Street Lighting (PJU-TS) with a lighting level of 3-6 lux resulting in a lamp wattage of 40 W, lamp working hours of 11 hours 14 minutes, solar module 300 WP, solar charge controller current 15.72 A, battery 40 Ah, battery working hours 13.72-18.68 hours, percentage of battery Ah usage 46.42% - 95%.%. In addition to meeting the standards of the Minister of Transportation of the Republic of Indonesia Number PM 27/2018, the results of this simulation also meet the Reliability Standard Power Plant recommendations with reliability exceeding 80%, namely 81.27% - 100%. While the PJU-TS of 21 units does not meet the standards of the Minister of Transportation of the Republic of Indonesia Number PM 27/2018 concerning Street Lighting Equipment and Reliability Standard Power Plant recommendations.

References

[1]   Ashariansyah, A., & Budiman, A. (2018). Perencanaan Penyediaan Daya Listrik Berbasis Tenaga Surya Untuk Penerangan Jalan Umum Di Kampus Universitas Borneo Tarakan. *Jurnal: Elektrika Borneo (JEB)*, *4*(2).

[2]   Nurrochim, A. (2018). "Perencanaan Lampu Penerangan Jalan Umum Tenaga Surya (LPJUTS) di Jalan

Laut Kendal. Universitas Semarang.

[3]   Pamungkas, I., Irawan, H. T., Arhami, A., & Dirhamsyah, M. (2019). Usulan Waktu Perawatan Dan Perbaikan Berdasarkan Keandalan Pada Bagian Boiler Di Pembangkit Listrik Tenaga Uap. *Jurnal Optimalisasi*, *5*(2), 82-95.

Biographies of Authors

	M. Tesar Apriliandy is an undergraduate student of Electrical Engineering Department, Borneo University Tarakan. He was a member of the Electrical Engineering Student Association for the 2019-2020 period.
	Achmad Budiman is an Electrical Engineering Lecturer since 2002. He obtained his Bachelor's degree in Electrical Engineering from Gadjah Mada University, Yogyakarta. He obtained his Master's degree in Electrical Engineering from ITS Surabaya. Currently, he serves as the Head of Electrical Engineering Study Program, Borneo Tarakan University. He is interested in the field of stability in power distribution and transmission systems.